Constitutionally Asymmetric and Chiral [2]Pseudorotaxanes[1]

Masumi Asakawa,[†] Peter R. Ashton,[†] Wayne Hayes,[†] Henk M. Janssen,[‡] E. W. Meijer,*[,‡] Stephan Menzer,[§] Dario Pasini,[†] J. Fraser Stoddart[⊥],*[,†,] Andrew J. P. White,[§] and David J. Williams*[,§]

Contribution from The School of Chemistry, The University of Birmingham, Edgbaston, Birmingham B15 2TT, U.K., The Laboratory of Organic Chemistry, Eindhoven University of Technology, 5600 MB Eindhoven, The Netherlands, and The Department of Chemistry, Imperial College, London SW7 2AY, U.K.

Received January 2, 1997. Revised Manuscript Received November 29, 1997

Abstract: The self-assembly and characterization of a range of chiral pseudorotaxanes has been explored using chiroptical methods. The syntheses of (i) constitutionally asymmetric acyclic hydroquinone-containing polyethers and (ii) optically active hydroquinone-containing acyclic polyethers, bearing pairs of methyl or isobutyl groups related to each other in a C_2-symmetric manner within the polyether backbone, are described. The combination of (i) the tetracationic cyclophane cyclobis(paraquat-*p*-phenylene) tetrakis(hexafluorophosphate), possessing a π-electron deficient cavity, and (ii) the linear noncentrosymmetric acyclic polyethers produces [2]pseudorotaxanes that have been characterized by ^{1}H NMR, UV/vis and circular dichroism (CD) spectroscopies in solution and by X-ray crystallography in the solid state. The introduction of constitutional asymmetry or chirality gives rise to a number of different geometries for the [2]pseudorotaxanes in both the solution and solid states. In particular, CD-spectroscopic measurements on the optically active [2]-pseudorotaxanes have shown that—depending on the positions of the C_2 symmetrically related chiral centers in the polyether chains with respect to the hydroquinone rings—the chirality present in the π-electron rich threadlike guest can induce chirality that is associated with the supramolecular structure as a whole, resulting in a chiral charge-transfer transition involving not only the π-donors in the chiral guests but also the π-acceptors in the achiral host.

Introduction

Nature employs numerous kinds of self-assembly processes[2] to construct large ordered molecular assemblies and supramolecular arrays. Employing the concept of self-assembly to construct functioning synthetic systems,[3] previously unattainable using conventional chemical techniques, the nature of specific recognition motifs is being investigated in both the solid and solution states.[4] Studies involving *divergently* and *convergently* arranged recognition motifs have led to the discovery of linear one-, two-, and three-dimensional solid-state arrays, incorporating hydrogen bonding,[5] metal−ligand complexes,[6] and $\pi-\pi$ interactions.[7] Investigations of the complexation of planar π-electron-deficient substrates [e.g., the paraquat dication] by the crown ether[8] bis(*p*-phenylene)-34-crown-10 (BPP34C10) have led to the self-assembly of interwoven and mechanically interlocked linear systems,[9] such as pseudorotaxanes and rotaxanes, respectively.

Several [*n*]pseudorotaxanes have been reported which incorporate cyclobis(paraquat-*p*-phenylene) $\mathbf{1}^{4+}$ (Figure 1) and linear π-electron-rich components.[10] They self-assemble in solution via a thermodynamically driven *threading* process to form remarkably stable species that are stabilized by (i) $\pi-\pi$ interactions[11] between the π-electron-deficient bipyridinium units of the cyclophane host and the π-electron-rich aromatic

[†] University of Birmingham.
[‡] Eindhoven University of Technology.
[§] Imperial College.
[⊥] Present address: Department of Chemistry and Biochemistry, University of California at Los Angeles, 405 Hilgard Avenue, Los Angeles, CA 90095. Phone: (310) 206-7078. FAX: (310) 206-1843. E-mail: stoddart@chem.ucla.edu.

(1) Molecular Meccano. 21. Part 20: Ashton, P. R.; Boyd, S. E.; Claessens, G. C.; Gillard, R. E.; Menzer, S.; Stoddart, J. F.; Tolley, M. S.; White, A. J. P.; Williams, D. J. *Chem. Eur. J.* **1997**, *3*, 788−798.

(2) For articles on chemical and biological self-assembly processes, see: (a) Jeffrey, G. A.; Saenger, W. *Hydrogen Bonding in Biological Structures* Springer-Verlag: Berlin, 1991. (b) Lindsey, J. S. *New J. Chem.* **1991**, *15*, 153−180. (c) Philp, D.; Stoddart, J. F. *Angew. Chem., Int. Ed. Engl.* **1996**, *35*, 1155−1196.

(3) For articles describing the potential use of self-assembly for the construction of nanoscale devices, see: (a) Bissell, R. A.; De Silva, A. P.; Gunaratne, H. Q. M.; Lynch, P. L. M.; Maguire, G. E. M.; Sandanayake, K. R. A. S. *Chem. Soc. Rev.* **1992**, *21*, 187−195. (b) Gómez-López, M.; Preece, J. A.; Stoddart, J. F. *Nanotechnology* **1996**, *7*, 183−192.

(4) For approaches to the design of supramolecular systems, see, for example: (a) Lehn, J.-M. *Angew. Chem., Int. Ed. Engl.* **1988**, *27*, 89−112. (b) Zaworotko, M. J. *Chem. Soc. Rev.* **1994**, *23*, 283−288. (c) Amabilino, D. B.; Stoddart, J. F.; Williams, D. J. *Chem. Mater.* **1994**, *6*, 1159−1167. (d) Desiraju, G. R. *Angew. Chem., Int. Ed. Engl.* **1995**, *34*, 2311−2327.

(5) For some recent examples of supramolecular systems assembled using hydrogen bonding, see: (a) Ghadiri, M. R.; Kobayashi, K.; Granja, J. R.; Chadha, R. K.; McRee, D. E. *Angew. Chem., Int. Ed. Engl.* **1995**, *34*, 93−95. (b) Boucher, É.; Simard, M.; Wuest, J. D. *J. Org. Chem.* **1995**, *60*, 1408−1412. (c) Glink, P. T.; Schiavo, C.; Stoddart, J. F. *Chem. Commun.* **1996**, 1483−1490. (d) Zimmerman, S. C.; Zeng, F. W.; Reichert, D. E. C.; Kolotuchin, S. V. *Science* **1996**, *271*, 1095−1098.

(6) For some recent examples of supramolecular systems assembled using metal−ligand interactions, see: (a) Goodgame, D. M. L.; Menzer, S.; Smith, A. M.; Williams, D. J. *Angew. Chem., Int. Ed. Engl.* **1995**, *34*, 574−575. (b) Beissel, T.; Powers, R. E.; Raymond, K. N. *Angew. Chem., Int. Ed. Engl.* **1996**, *35*, 1084−1086.

(7) For supramolecular systems assembled using $\pi-\pi$ interactions, see: (a) Ashton, P. R.; Ballardini, R.; Balzani, V.; Belohradsky, M.; Gandolfi, M. T.; Philp, D.; Prodi, L.; Raymo, F. M.; Reddington, M. V.; Spencer, N.; Stoddart, J. F.; Venturi, M.; Williams, D. J. *J. Am. Chem. Soc.* **1996**, *118*, 4931−4951 and references cited therein.

(8) Allwood, B. L.; Spencer, N.; Shahriari-Zavareh, H.; Stoddart, J. F.; Williams, D. J. *J. Chem. Soc., Chem. Commun.* **1987**, 1064−1066.

(9) Amabilino, D. B.; Stoddart, J. F. *Chem. Rev.* **1995**, *95*, 2725−2828.

S0002-7863(97)00018-8 CCC: $15.00 © 1998 American Chemical Society
Published on Web 01/27/1998

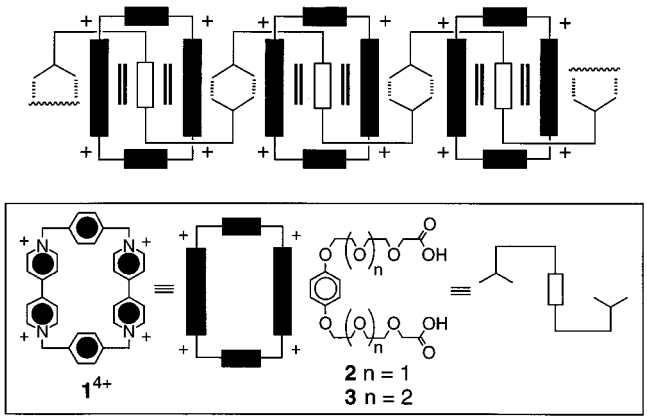

Figure 1. Schematic representation of the solid-state structure of the 1:1 complexes formed between the tetracationic cyclophane **1**·4PF_6 and the π-electron-rich dicarboxylic acid components **2** and **3**.

residues of the linear guest, (ii) [CH···O] hydrogen bonds[12] between the α-bipyridinium protons on the tetracationic cyclophane and polyether oxygen atoms in the linear π-electron-rich guest, and (iii) [CH···π] interactions[13] between the aromatic ring protons of the included π-electron-rich aromatic residues and the π-face of the *p*-xylyl spacer units of the tetracationic cyclophane. In addition, complex infinite supramolecular arrays are evident in the solid state.

Recently, we reported[14] the self-assembly (Figure 1) of pseudorotaxanes comprised of the tetracationic cyclophane $\mathbf{1}^{4+}$ and the π-electron-rich polyethers **2** and **3**, possessing carboxylic acid termini. In these superstructures, the "threads" are inserted centrosymmetrically into the π-electron-deficient cavity of the cyclophane, and in the solid state, they self-assemble further in a supramolecular fashion as a result of hydrogen-bonding interactions between the carboxylic acid termini[15] to produce pseudopolyrotaxanes.[16] To verify the generality and the viability of this noncovalent synthesis of pseudopolyrotaxanes, we have introduced (i) constitutional asymmetry into the π-electron-rich thread components by replacing one of the carboxylic acid functionalities and (ii) chirality in the form of C_2-related chiral centers within the polyether backbone of the threads. The introduction of chirality into the linear thread component could, in principle, lead to the formation of *helical* polymeric superstructures.[17] Additionally, the dissymmetry associated with these chiral threads can be used to study the geometry of the [2]pseudorotaxanes in solution by employing circular dichroism (CD) spectroscopy.

Here we describe (i) the syntheses of the thread components featuring a range of terminal functionalities and chiralities, (ii) the characterization of a series of [2]pseudorotaxanes incorporating constitutionally asymmetric and chiral thread components and **1**·4PF_6 *in solution* by UV/vis, ^{1}H NMR, and CD spectroscopic studies, and (iii) their characterization in the *solid state* by X-ray crystallography.

Scheme 1

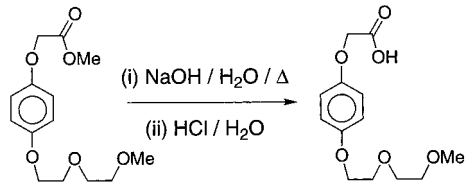

Results and Discussion

Synthesis of the Molecular Components. Compound **5** was prepared (Scheme 1) from the methyl ester **4**.[18]

The *chiral* π-electron-rich aromatic dicarboxylic acid components were prepared by the routes shown in Schemes 2−4. The (*S*)-compounds (Scheme 2) have been reported previously.[19] The (*R*)-enantiomers were synthesized employing analogous procedures. Using the shown synthetic route, the optical purities of the starting compounds, leucine (*S*)-**6**, lactide (*RR*)-**7**, and ethyl lactate (*S*)-**9**, could be preserved through to the final compounds.[19d]

The diols *(SS)*-**19** and *(RR)*-**19** were prepared (Scheme 3) by *O*-alkylation of **16** with the tosylates *(S)*-**15** and *(R)*-**15**, respectively. Coupling of the bistosylates **17** and **18**[20] with the THP-protected diols **13** and **14** and subsequent deprotection of the THP protecting groups afforded the C_2-symmetric chiral polyethers **20**−**23**. *O*-Alkylation of diols **19**−**23** with *tert*-butyl bromoacetate yielded the *tert*-butyl diesters **24**−**28** in 31−45%

(10) For reports of pseudorotaxanes incorporating π-electron-rich linear threads and cyclobis(paraquat-*p*-phenylene), see: (a) Ashton, P. R.; Philp, D.; Spencer, N.; Stoddart, J. F.; Williams, D. J. *J. Chem. Soc., Chem. Commun.* **1994**, 181−184. (b) Castro, R.; Berardi, M. J.; Córdova, E.; Ochoa de Olza, M.; Kaifer, A. E.; Evanseck, J. D. *J. Am. Chem. Soc.* **1996**, *118*, 10257−10268. For reports of pseudorotaxanes incorporating π-electron-deficient bipyridinium guests and BPP34C10 as the host, see: (a) Ashton, P. R.; Philp, D.; Reddington, M. V.; Slawin, A. M. Z.; Spencer, N.; Stoddart, J. F.; Williams, D. J. *J. Chem. Soc., Chem. Commun.* **1991**, 1680−1683. (b) Shen, Y. X.; Engen, P. T.; Berg, M. A. G.; Merola, J. S.; Gibson, H. W. *Macromolecules* **1992**, *25*, 2786−2788.

(11) $\pi-\pi$ interactions have been described in the following recent publications: (a) Diederich, F.; Philp, D.; Seiler, P. *J. Chem. Soc., Chem. Commun.* **1994**, 205−208. (b) Bilyk, A.; Harding, M. M.; Turner, P.; Hambley, T. W. *J. Chem. Soc., Dalton Trans.* **1994**, 2783−2790. (c) Otsuki, J.; Oya, T.; Lee, S.-H.; Araki, K. *J. Chem. Soc., Chem. Commun.* **1995**, 2193-2194.

(12) For reviews describing experimental evidence and theoretical aspects of [CH···O] hydrogen bonding, see: (a) Desiraju, G. R. *Acc. Chem. Res.* **1991**, *24*, 290−296. (b) Steiner, T. *Chem. Commun.* **1997**, 727−734.

(13) For a review describing [CH···π] interactions, see: Nishio, M.; Umezawa, Y.; Hirota, M.; Takeuchi, Y. *Tetrahedron* **1995**, *32*, 8665−8701.

(14) Asakawa, M.; Ashton, P. R.; Brown, G. R.; Hayes, W.; Menzer, S.; Stoddart, J. F.; White, A. J. P.; Williams, D. J. *Adv. Mater.* **1996**, *8*, 37−41.

(15) For articles describing the assembly of hydrogen-bonded linear systems featuring the carboxylic acid−carboxylic acid recognition motif, see: (a) Hoshino, H.; Jin, J. I.; Lenz, R. W. *J. Appl. Polym. Sci.* **1984**, *29*, 547−554. (b) Zhao, Y.-L.; Fowler, F. W.; Lauher, J. W. *J. Am. Chem. Soc.* **1990**, *112*, 6627−6634. (c) Lillya, C. P.; Baker, R. J.; Hütte, S.; Winter, H. H.; Lin, Y.-G.; Shi, J.; Dickenson, L. C.; Chien, J. C. W. *Macromolecules* **1992**, *25*, 2076−2080.

(16) *Pseudopolyrotaxanes* have been defined as polymeric structures that are comprised of a linear macromolecule which incorporates numerous macrocycles along its length, whereas *polypseudorotaxanes* are defined as a covalently linked array of pseudorotaxanes, where the macrocycles are not confined on the polymer backbone, but rather are located on strands emanating from the polymer backbone. See: (a) Amabilino, D. B.; Stoddart, J. F. *Pure Appl. Chem.* **1993**, *65*, 2351−2359. (b) Marsella, M. J.; Carroll, P. J.; Swager, T. M. *J. Am. Chem. Soc.* **1994**, *117*, 9832−9841.

(17) For articles describing an induction of chirality into polymeric systems, see: (a) Zarges, W.; Hall, J.; Lehn, J.-M.; Bolm, C. *Helv. Chim. Acta* **1991**, *74*, 1843−1852. (b) Gulik-Krzywicki, T.; Fouquey, C.; Lehn, J.-M. *Proc. Natl. Acad. Sci. U.S.A.* **1993**, *90*, 163−167.

(18) Asakawa, M.; Ashton, P. R.; Menzer, S.; Raymo, F. M.; Stoddart, J. F.; White, A. J. P.; Williams, D. J. *Chem. Eur. J.* **1996**, *2*, 877−893.

(19) (a) Perkins, M. V.; Kitching W.; König, W. A.; Drew, R. A. I. *J. Chem. Soc., Perkin Trans. 1* **1990**, 2501−2506. (b) Cowie, J. M. G.; Hunter, H. W. *Makromol. Chem.* **1990**, *191*, 1393−1402. (c) Mori, K. *Tetrahedron* **1976**, *32*, 1101−1105. (d) Koppenhoefer, B.; Trettin, U.; Figura, R.; Lin, B. *Tetrahedron Lett.* **1989**, *38*, 5109−5110. In a test, *(R)*-1,2-propanediol was stirred overnight under basic conditions (KOH/dioxane) and checked on a permethylated β-cyclodextrin GC column. Comparison with *(S)*-1,2-propanediol showed that no racemization had taken place.

(20) Anelli, P. L.; Ashton, P. R.; Ballardini, R.; Balzani, V.; Delgado, M.; Gandolfi, M. T.; Goodnow, T. T.; Kaifer, A. E.; Philp, D.; Pietraszkiewicz, M.; Prodi, L.; Reddington, M. V.; Slawin, A. M. Z.; Spencer, N.; Stoddart, J. F.; Vicent, C.; Williams, D. J. *J. Am. Chem. Soc.* **1992**, *114*, 193-218.

Scheme 2

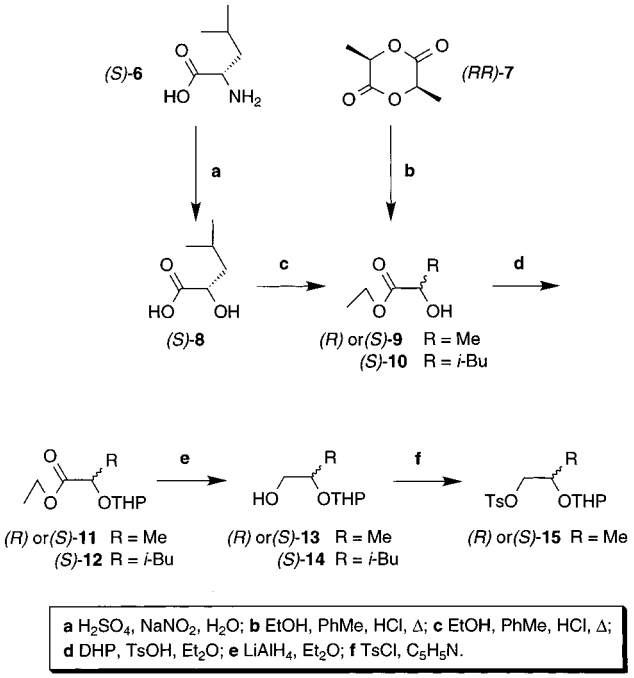

a H_2SO_4, $NaNO_2$, H_2O; **b** EtOH, PhMe, HCl, Δ; **c** EtOH, PhMe, HCl, Δ; **d** DHP, TsOH, Et_2O; **e** $LiAlH_4$, Et_2O; **f** TsCl, C_5H_5N.

Scheme 3

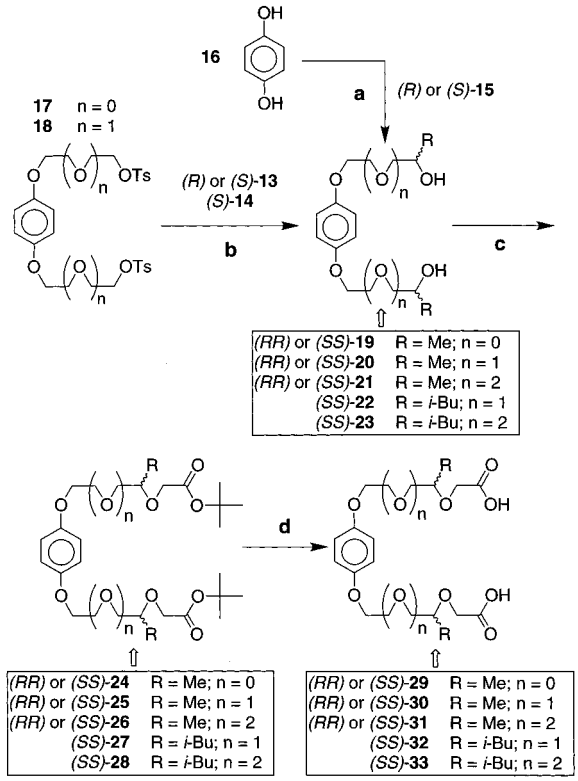

a (i) KOH, THF, EtOH, Δ; (ii) TsOH, MeOH; **b** (i) KOH, THF, Δ; (ii) TsOH, MeOH; **c** $BrCH_2CO_2t$-Bu, *t*-BuOK, *t*-BuOH; **d** TFA, CH_2Cl_2 or TFA or HX (X = Cl, Br), CH_2Cl_2.

yields. Hydrolysis of these diesters afforded the dicarboxylic acids **29**−**33** in quantitative yields. Remarkably, the specific optical rotations of these acids were not reliable for determining the enantiomeric excesses, because the $[\alpha]_D$ values are very sensitive to changes in temperature, concentration, and solvent.

Compound *(SS)*-**34** was prepared (Scheme 4) by coupling of hydroquinone **16** with the tosylate[21] of *(S)*-2-methylbutanol. The diols *(SS)*-**19** and *(RR)*-**19** were transformed with MeI into the

Scheme 4

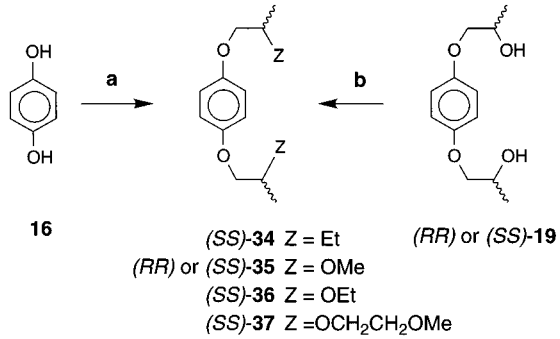

a *(S)*-$TsOCH_2CHMeEt$, KOH, THF, EtOH, Δ; **b** MeI, *t*-BuOK, *t*-BuOH or EtI, KOH, THF, Δ or $TsOCH_2CH_2OMe$, KOH, THF, Δ.

dimethoxy ethers *(SS)*-**35** and *(RR)*-**35**. Similarly, the diol *(SS)*-**19** was converted to the ethers *(SS)*-**36** and *(SS)*-**37** by reaction with EtI and the tosylate[22] of 2-methoxyethanol, respectively.

^{1}H NMR Spectroscopy. Mixing equimolar proportions of **1**·4PF_6 and separately each of the π-electron-rich threads in MeCN produced bright red solutions of the respective 1:1 complexes. The formation of these colors indicates that the threads enter the cavity of the tetracationic cyclophane and experience stabilizing π−π interactions. The chemical shift changes observed (Table 1) for protons in the 1:1 complexes **2**/**1**·4PF_6 and **3**/**1**·4PF_6, with respect to free **1**·4PF_6 and the polyethers **2** or **3** as reference compounds, are consistent with those found[20] for similar 1:1 complexes employing **1**·4PF_6 as the host.

However, the two 1:1 complexes **2**/**1**·4PF_6 and **3**/**1**·4PF_6 do not exhibit the same spectroscopic behavior. There are significant differences between the resonances of the methylene protons adjacent to the carboxylic acid termini in the polyether chains of these 1:1 complexes in comparison with those for the same protons in the free polyethers **2** and **3** in CD_3CN solution. In **3**/**1**·4PF_6, the methylene protons resonate with a significant upfield shift ($\Delta\delta = -0.17$ ppm), implying, on a time-averaged basis, that these protons are oriented directly over the bipyridinium unit of the tetracationic cyclophane and are subsequently shielded, whereas in **2**/**1**·4PF_6, the methylene proton resonances undergo a downfield shift ($\Delta\delta = +0.12$ ppm), indicating that the termini of the polyether chains must be lying in the same plane as the bipyridinium protons of the tetracationic cyclophane.

Similar behavior was observed during the ^{1}H NMR spectroscopic studies of the methyl-substituted chiral pseudorotaxanes **29**/**1**·4PF_6, **30**/**1**·4PF_6, **31**/**1**·4PF_6,[23] and the isobutyl-substituted analogues **32**/**1**·4PF_6 and **33**/**1**·4PF_6. However, a comparison of the spectroscopic behavior of the two 1:1 complexes **30**/

(21) Hahn, B.; Percec, V. *Macromolecules* **1987**, *20*, 2961−2968.

(22) Ouchi, M.; Inoue, Y.; Liu, Y.; Nagamune, S.; Nakamura, S.; Wada, K.; Hakushi, T. *Bull. Chem. Soc. Jpn.* **1990**, *63*, 1260−1262.

(23) The hydroquinone ring proton resonances of the included π-electron-rich components in the 1:1 complexes **2**−**3**/**1**·4PF_6 and **29**−**31**/**1**·4PF_6 could not be assigned at room temperature in CD_3CN solutions, as a result of appreciable broadening attributable to fast complexation−decomplexation processes on the ^{1}H NMR time scale. In the 1:1 complexes **2**/**1**·4PF_6 and **3**/**1**·4PF_6, the hydroquinone ring proton resonances were located at δ 3.74 and 3.75 by saturation transfer experiments in CD_3COCD_3 at 243 and 233 K, respectively, in comparison with δ 6.69 and 6.71 for free **2** and **3**. The upfield shifts for the hydroquinone ring proton resonances (Δδ −2.95 and −2.96 ppm, respectively) are consistent with findings of variable temperature ^{1}H NMR spectroscopic investigations of similar complexes and mechanically interlocked systems; see ref 20.

Table 1. Chemical Shift Data [δ Values ($\Delta\delta$ Values)][a] Obtained from the 300 MHz ^{1}H NMR Spectra Recorded on 1:1 Complexes Formed between the π-Electron-Rich Aromatic Polyethers and the Tetracationic Cyclophane **1**·4$PF_6$and Their Components in CD_3CN Solution at 298 K

compound or 1:1 complex	charged component				polyether component	
	α-CH	β-CH	C_6H_4	CH_2N^+	ArH	CH_2CO
1·4PF_6[b]	8.86	8.16	7.52	5.74		
2					6.85	4.08
2/**1**·4PF_6	8.91	7.90	7.74	5.70	ND[c]	4.29
	(0.05)	(−0.26)	(0.22)	(−0.04)		(0.12)
3					6.84	4.06
3/**1**·4PF_6	8.91	7.90	7.73	5.72	ND[c]	3.89
	(0.05)	(−0.26)	(0.21)	(−0.02)		(−0.17)
5					6.84	4.57
5/**1**·4PF_6	8.88	8.02	7.67	5.73	5.28 (−1.56)	4.48
	(0.02)	(−0.14)	(0.15)	(−0.01)	5.21 (−1.63)	(−0.09)
29					6.84	4.11
29/**1**·4PF_6	8.91	8.02	7.65	5.73	ND[c]	4.28
	(0.05)	(−0.14)	(0.13)	(−0.01)		(0.17)
30					6.85	4.11
30/**1**·4PF_6	8.89	8.01	7.66	5.72	ND[c]	4.18
	(0.03)	(−0.15)	(0.14)	(−0.02)		(0.07)
31					6.85	4.15
31/1·4PF_6	8.88	7.97	7.69	5.72	ND[c]	4.06
	(0.02)	(−0.19)	(0.17)	(−0.02)		(−0.04)
32						
32/**1**·4PF_6[d]	8.86 (0.00)	8.16 (0.00)	7.52 (0.00)	5.74 (0.00)	6.85	4.15 (0.00)
	8.92 (0.06)	7.86 (−0.30)	7.80 (0.28)	5.72 (−0.02)	(0.00)	4.30 (0.15)
33					6.84	4.13
33/**1**·4PF_6[d]	8.86 (0.00)	8.15 (−0.01)	7.53 (0.01)	5.74 (0.00)	6.84	4.13 (0.00)
	8.89 (0.03)	7.86 (−0.30)	7.79 (0.27)	5.72 (−0.02)	(0.00)	4.10 (−0.03)
34					6.84	
34/**1**·4PF_6	8.87	8.14	7.58	5.77	6.41	
	(0.01)	(−0.02)	(0.06)	(0.03)	(−0.43)	

[a] The $\Delta\delta$ values indicated in parentheses under the respective δ values relate to the changes in chemical shift exhibited by the probe protons upon complex formation. A negative value indicates the movement of the resonance to high field. [b] See ref 20. [c] For these complexes, the hydroquinone ring proton resonances at 298 K in CD_3CN are broad under the baseline. See refs 23. [d] For these complexes, exchange between the 1:1 complex and free components is slow on the ^{1}H NMR time scale, thus resulting in the observation of "free" and complexed cyclophane proton resonances in these spectra at 298 K. See the text for details.

1·4PF_6 and **32**/**1**·4PF_6 revealed important differences. In the ^{1}H NMR spectrum (Figure 2a) of **30**/**1**·4PF_6, there were no significant differences compared with the ^{1}H NMR spectrum of 1:1 complex **2**/**1**·4PF_6. Time-averaged signals—as a result of fast exchange between complexed and uncomplexed states—were observed. In contrast, in the ^{1}H NMR spectrum (Figure 2b) of **32**/**1**·4PF_6, sets of resonances could be identified for complexed **1**·4PF_6 and the complexed isobutyl-substituted chiral thread **32**, along with another set for free **1**·4PF_6 and free **32**.[24] The same spectroscopic behavior was observed for **33**/**1**·4PF_6, thus confirming that the introduction of bulky isobutyl groups into the polyether chains slows the rate of the threading−unthreading process involving **1**·4PF_6, presumably because of steric and conformational effects in solution.[25]

Stability Constants of [2]Pseudorotaxanes. The stability constants and derived free energies for the formation of [2]-pseudorotaxanes between **1**·4PF_6 and **2**, **3**, **5**, and **29**−**34** were obtained (Table 2) by UV/vis spectroscopic titrations[26] in MeCN at 25 °C. Using the charge-transfer (CT) band as the probe, stability constants (K_a) of 1900 and 1800 M^{-1} for **2**/**1**·4PF_6 and **3**/**1**·4PF_6, respectively, were obtained. They correspond to free energies of complexation ($\Delta G°$) for **2**/**1**·4PF_6 and **3**/**1**·4PF_6 of −4.5 and −4.4 kcal mol^{-1}, respectively—values that are of the same magnitudes as those already obtained[20] for similar 1:1 complexes. On the other hand, for the methyl or isobutyl-substituted diacids **29**−**33**, the K_a and $\Delta G°$ values for [2]-pseudorotaxane formation are clearly reduced to values in the range 170−900 M^{-1}, i.e., from −3.0 to −4.0 kcal mol^{-1}, respectively, indicating that the introduction of bulky groups within the polyether regions of the threads lowers the relative thermodynamic stabilities of the resulting pseudorotaxanes, probably because of steric and conformational effects. Surprisingly, the stability constant (K_a = 1800 M^{-1}) and free energy ($\Delta G°$ = −4.4 kcal mol^{-1}) of the [2]pseudorotaxane formation for **5**/**1**·4PF_6 are of the same magnitude as those found for **2**/**1**·4PF_6 and **3**/**1**·4PF_6, indicating a possible stabilizing interaction between the carboxylic acid functionality and the acidic hydrogen atoms of the tetracationic cyclophane, which in **5**/**1**·4PF_6, are in close proximity.[27] The association constant (24 M^{-1}) for **34**/**1**·4PF_6 is similar to that (17 M^{-1}) reported in the literature[20] for the 1:1 complex formed between 1,4-dimethoxybenzene and **1**·4PF_6.

X-ray Crystallography. Crystals of the monocarboxylic acid **5** contain two crystallographically independent molecules **A** and **B** in the asymmetric unit, both having virtually identical

(24) In **32**/**1**·4PF_6 and **33**/**1**·4PF_6, the ratios between complexed **1**·4PF_6 and free **1**·4PF_6 in CD_3CN at 298 K were 35:65 and 62:38, respectively, as measured from integrations of the resonances assigned to the β-bipyridinium and *p*-xylyl ring protons on the tetracationic cyclophane **1**·4PF_6 in the ^{1}H NMR spectrum. The stability constants (K_a) of the complexes could be obtained from the ratios of complexed and uncomplexed components.

(25) This situation is reminiscent of a synthetic approach to self-assembling [*n*]rotaxanes we refer to as "slippage". The approach relies upon the complementarity between π-electron-deficient bipyridinium-based dumbbell-shaped components and π-electron-rich hydroquinone-based or dioxynaphthalene-based macrocyclic polyether components. By careful selection of the size of the stoppers covalently attached at both ends of the dumbbell-shaped compounds, together with the size of the macrocyclic polyethers, the association of the complementary components to afford rotaxanes can be achieved under the influence of thermal energy. See: Asakawa, M.; Ashton, P. R.; Balzani, V.; Belohradsky, M.; Gandolfi, M. T.; Kocian, O.; Prodi, L.; Raymo, F. M.; Stoddart, J. F.; Venturi, M. *J. Am. Chem. Soc.* **1996**, *118*, 12012−12020.

(26) Connors, K. A. *Binding Constants*; Wiley: New York, 1987.

(27) Benniston, A. C.; Harriman, A. *Synlett* **1993**, *3*, 223−226.

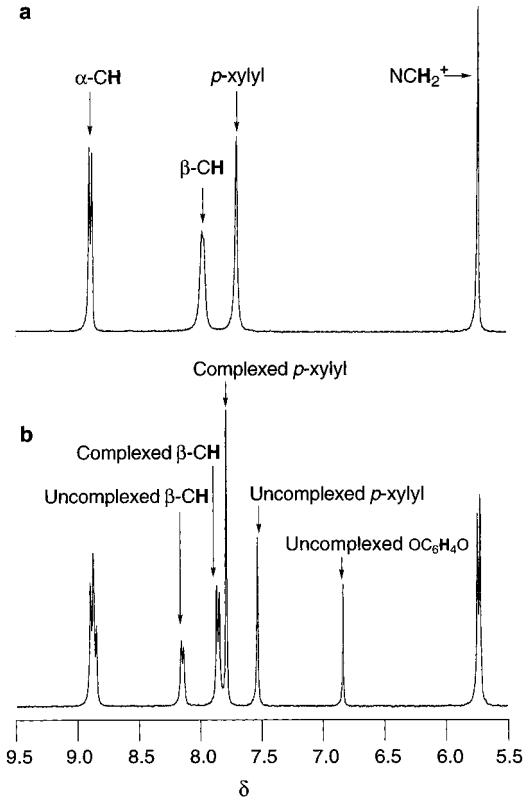

Figure 2. Partial ^{1}H NMR spectra of the pseudorotaxane complexes (a) **30**/**1**·4PF$_6$, and (b) **32**/**1**·4PF$_6$ in CD_3CN at 298 K. The concentrations of all components, **1**·4PF$_6$, **30**, and **32**, was 5 mM.

Table 2. Stability Constants for [2]Pseudorotaxanes

[2]pseudorotaxane	λ_{max} (nm)[a]	K_a (M^{-1})	$-\Delta G°$ (kcal mol^{-1})[b]
2/**1**·4PF$_6$	467	1900	4.5
3/**1**·4PF$_6$	467	1800	4.4
5/**1**·4PF$_6$	453	1800	4.4
29/**1**·4PF$_6$	460	320	3.4
30/**1**·4PF$_6$	461	310	3.4
31/**1**·4PF$_6$	464	860	4.0
32/**1**·4PF$_6$	463	170[c]	3.0
33/**1**·4PF$_6$	467	900[c]	4.0
34/**1**·4PF$_6$	476	24	1.9

[a] Tetrakis(hexafluorophosphate) salt in MeCN solution at 298 K. [b] Calculated from values of K_a. [c] Calculated from the ratios of integrations of ^{1}H NMR spectra of 1:1 complexes. See ref 24.

conformations. Both **A** and **B** type molecules form head-to-tail hydrogen-bonded macrocycles with their C_i-related counterparts (Figure 3), the carboxylic hydrogen atom in one molecule being hydrogen-bonded to the second oxygen atom of the polyether chain of the other and vice versa.[28] They are supplemented by a further pair of weaker [CH···π] interactions between one of the phenoxymethylene hydrogen atoms in one molecule and the hydroquinone ring in the other and vice versa.[29] There is a marginal overlap between the two coplanar hydroquinone rings.[30] The **A** and **B** type dimer pairs form zigzag stacks, with one of the hydroquinone hydrogen atoms of **A** type pairs being directed orthogonally into the face of the

(28) The geometries of these hydrogen-bonding interactions in type **A** and type **B** dimer pairs are, respectively, [O···O] distance 2.76 Å, [OH···O] distance 1.94 Å, and [OH···O] angle 152° and [O···O] distance 2.77 Å, [OH···O] distance 2.00 Å, and [OH···O] angle 144°.

(29) The geometries of T-type aromatic−aromatic edge-to-face interaction within type **A** and type **B** dimer pairs are, respectively, [H···π] distance 2.81 Å, [CH···π] angle 143°, and [H···π] vector inclined by 85° to the ring plane and [H···π] distance 2.79 Å, [CH···π] angle 145°, [H···π] vector inclined by 85° to the ring plane.

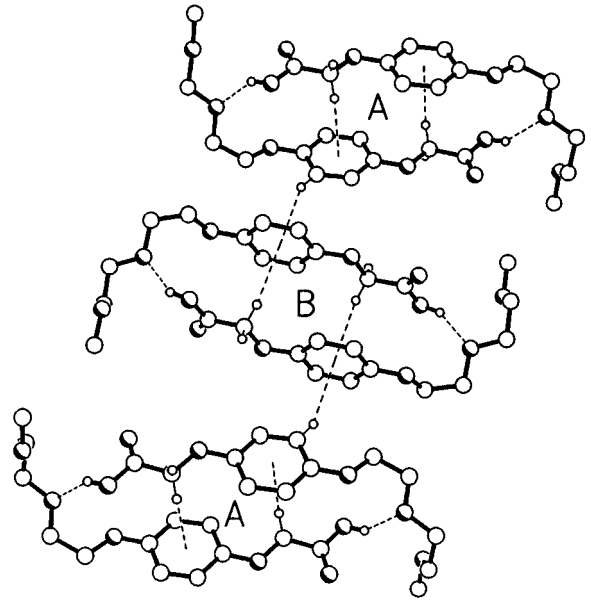

Figure 3. Supramolecular packing of the hydrogen-bonded macrocycles **A** and **B** in the solid-state structure of **5**.

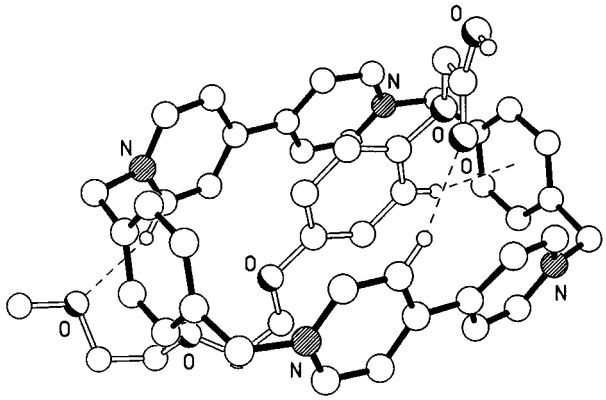

Figure 4. X-ray crystal structure of the [2]pseudorotaxane **5**/**1**·4PF$_6$.

hydroquinone ring of a **B** type pair via a T-type aromatic−aromatic edge-to-face interaction ([H···π] distance 2.69 Å, [CH···π] angle 145°, [H···π] vector inclined by 76° to the ring plane). The inter- and intramolecular [H..π] vectors subtend an angle of 177°. Adjacent lattice-translated stacks are oriented such that one of the phenoxymethylene CH groups of **B** type pairs of molecules (that are not involved in intradimer [CH···π] interactions) are directed into the opposite face of the hydroquinone rings of **A** type molecules to form a [CH···π] interaction [**B** to **A** type] complementary to that within the **A** to **B** type dimer pairs ([H···π] distance 2.76 Å, [CH···π] angle 132°, [H···π] vector inclined by 85° to the ring plane). Here, the inter- and intramolecular [H···π] vectors subtend an angle of 171°.

In **5**/**1**·4PF$_6$, the thread is inserted (Figure 4) through the center of the tetracation. In addition to $\pi-\pi$ stacking interactions, the complex is stabilized by a pair of [CH···O] hydrogen bonds between (a) one of the β-CH bipyridinium hydrogen atoms and the carboxyl carbonyl oxygen atom ([C···O] distance 3.20 Å, [H···O] distance 2.30 Å, [CH···O] angle 156°) and (b) one of the α-bipyridinium hydrogen atoms and the third oxygen atom of the polyether chain ([C···O] distance 3.38 Å, [H···O] distance 2.47 Å, [OH···O] angle 159°). There is also a [CH···π]

(30) The distances between the aromatic rings within the type **A** and type **B** dimer pairs are, respectively, mean interplanar separations 3.56 Å and centroid−centroid distance 4.93 and 4.92 Å.

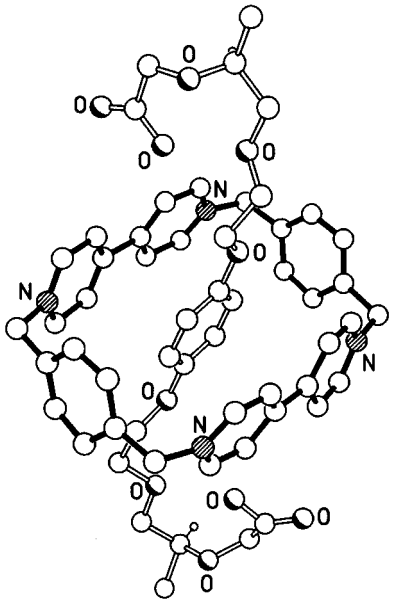

Figure 5. X-ray crystal structure of the [2]pseudorotaxane *(SS)*-**30**/**1**·4PF_6.

interaction[31] between one of the hydroquinone hydrogen atoms and one of the *p*-xylyl rings of the tetracation ([H···π] distance 2.70 Å, [CH···π] angle 166°).

The packing of the 1:1 complexes shows the threads to be linked head-to-tail via a strong [H···O] hydrogen bond between the hydrogen atom of the carboxylic unit of one of the threads and the third oxygen atom of the polyether chain of the next chain ([O···O] distance 2.77 Å, [H···O] distance 1.87 Å, [OH···O] angle 176°), thereby forming a hydrogen-bonded pseudopolyrotaxane structure.

In the structure of the [2]pseudorotaxane *(SS)*-**30**/**1**·4PF_6, the chiral thread *(SS)*-**30** is inserted (Figure 5) through the center of the tetracation. An unusual feature of note is the adoption of a syn geometry by the two phenoxymethylene carbon atoms, requiring the O−C_6H_4−O axis of the hydroquinone ring to be more steeply inclined (76°) to the mean plane of the cyclophane; cf. that observed, for example, in the previous structure (48°), and in related systems.[20] This tilt weakens the [H···π] interactions between diametrically opposite hydroquinone ring hydrogen atoms and the *p*-xylyl rings of the tetracation. These distances are increased to ca. 3 Å; cf. values of ca. 2.8 Å in other hydroquinone-containing related systems.[20] On account of high thermal vibration parameters, the positions of the carboxyl hydrogen atoms could not be located, and so any hydrogen-bonding interactions involving these groups can only be inferred from contact distances between the oxygen centers. These contacts reveal the possibility of [CH···O] interactions between the β-CH hydrogen atoms of the bipyridinium units and one of the oxygen atoms of each of the carboxylate groups. Indeed, the orientation of the carboxylate group directly over the β-bipyridinium hydrogen atoms precludes, on steric grounds, a normal "in line" geometry for the carboxylate hydrogen atoms. However, one of the oxygen atoms of each carboxylate (that with the longer C−O bond) lies within intramolecular hydrogen-bonding distance of the second oxygen atom (relative to the hydroquinone ring) of the polyether chains, thereby providing

(31) The [CH···π] interaction is accompanied by a noticeable offset of the hydroquinone ring toward the interacting *p*-xylyl ring relative to the other. The hydroquinone ring, which is ca. 3.5 Å from the two bipyridinium units, is tilted by 48° with respect to the mean plane of the tetracationic cyclophane and shifted by ca. 0.25 Å toward one of the *p*-xylyl rings.

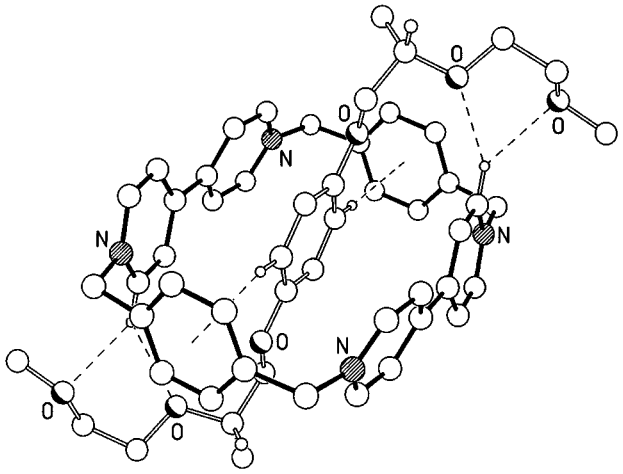

Figure 6. X-ray crystal structure of the [2]pseudorotaxane *(SS)*-**37**/**1**·4PF_6.

a possible explanation for the folded geometry observed for the thread. There are no intercomplex $\pi-\pi$ stacking or hydrogen-bonding interactions.

In *(SS)*-**37**/**1**·4PF_6, the polyether is threaded through the cavity of the cyclophane in an approximately centrosymmetric fashion, the exception being the methyl groups on the two chiral centers (see Figure 6). The absolute configurations of these two asymmetric carbon atoms have been unambiguously determined as being both *(S)* by crystallographic means. The hydroquinone ring of the polyether thread is sandwiched between the two π-electron-deficient bipyridinium units, with the distances separating the hydroquinone ring centroid and the centroid of the C−C bond linking the pyridinium rings being 3.55 and 3.57 Å. The −OC_6H_4O− axis of the hydroquinone ring is inclined to the mean plane of the tetracationic cyclophane (as defined by its four methylene carbon atoms) by ca. 52°, with the phenoxymethylene groups adopting an anti geometry. These data contrast with the [2]pseudorotaxane *(SS)*-**30**/**1**·4PF_6, where the angle is much steeper (76°). Consequently, the [H···π] interactions observed here between diametrically opposite hydroquinone hydrogen atoms and the *p*-xylyl rings of the cyclophane are of more usual lengths at distances of ca. 2.8 Å. The $\pi-\pi$ stacking interactions are supplemented by two pairs of bifurcated [CH···O] hydrogen bonds between the second and the third oxygen atoms of each polyether chain and one of the adjacent α-CH bipyridinium hydrogen atoms.[32] An inspection of the packing of the molecules reveals the presence of pairs of relatively weak [CH···π] interactions between one of the methylene carbon atoms of the polyether chain of one [2]-pseudorotaxane and a *p*-xylyl ring of the tetracation of a lattice-translated [2]pseudorotaxane counterpart, forming loosely linked chains that extend in the crystallographic *c*-direction.

The [2]pseudorotaxane solid-state structures of **2**/**1**·4PF_6 and **3**/**1**·4PF_6 reveal that all "programmed information" in the system—charge-transfer interactions, hydrogen bonding, and T-type interactions—is used to construct the crystal lattice. As evidenced by the crystal data on **5**/**1**·4PF_6, (*SS*)-**30**/**1**·4PF_6, and (*SS*)-**37**/**1**·4PF_6, the introduction of constitutional asymmetry or chirality in the π-electron-rich threads (i) results in a diversity of [2]pseudorotaxane structural features, i.e., the thread and **1**·4PF_6 can be assembled in various ways, and (ii) produces a variety of different packing motifs in the solid state. However,

(32) The [C···O] and [H···O] distances and [CH···O] angles for the four hydrogen bonds are 3.18 and 2.34 Å, 146°; 3.32 and 2.53 Å, 139°; 3.21 and 2.40 Å, 142°; and 3.24 and 2.43 Å, 141°, respectively.

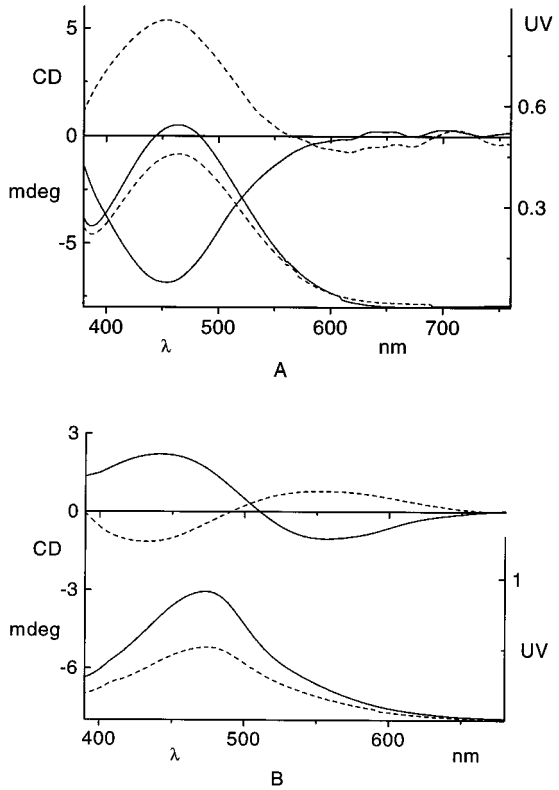

Figure 7. (a) CD and UV spectra for pseudorotaxanes *(SS)*-**29**/**1**·4PF_6 (solid) and *(RR)*-**29**/**1**·4PF_6 (dashed) in MeCN at 24 °C. (b) CD and UV spectra for pseudorotaxanes *(SS)*-**19**/**1**·4PF_6 (solid) and *(RR)*-**19**/**1**·4PF_6 (dashed) in MeCN at 24 and 20 °C, respectively.

this chirality or asymmetry has not led to an asymmetric packing in the supramolecular array; e.g., one-handed *helical* conformations of hydrogen-bonded chiral threads, for instance, are not observed. Consequently, refined crystal engineering is not readily possible with these asymmetric [2]pseudorotaxane systems, though results[14] for the symmetric analogues **2**/**1**·4PF_6 and **3**/**1**·4PF_6 are encouraging examples in this respect.

CD Measurements.[33] Circular dichroism measurements were performed in order to study the geometries of the pseudorotaxanes in solution. The measurements were conducted in the wavelength region of the CT band (400−600 nm), where the absorbance of the pseudorotaxane can be studied separately from the absorbance of noncomplexed material. Both CD and UV spectra of the solutions were taken to determine the *g* values of the observed CD effects.[34]

$$g_\lambda = (\Delta\epsilon/\epsilon)_\lambda = (\Delta A/A)_\lambda = \psi_\lambda/(32980A_\lambda)$$

The dicarboxylic acids **29**−**31** were investigated initially. Induced chirality in the CT band could only be observed for the enantiomers *(RR)*-**29** and *(SS)*-**29**. The observed CD effects are shown in Figure 7A. The g_{450} values of the induced CD effects were -3.9×10^{-4} and 3.7×10^{-4} for the (*SS*)- and the (*RR*)-threads, respectively.[35] These results show that the chiral centers of the threads must be close to the hydroquinone ring—closer than the second oxygen atom of the polyether chain relative to this ring—to give a complex with a "chiral geometry" and thus to influence the electronic transition in the CT band. To confirm these initial observations, additional CD measurements were performed on the threads **19** and **20**. In line with the previous results, *(RR)*-**20** did not and *(RR)*-**19** and *(SS)*-**19** did show induced CD effects in the CT band (see Figure 7B).

However, the nature of the observed (Figure 7B) CD effects for the complexes *(SS)*-**19**/**1**·4PF_6 and *(RR)*-**19**/**1**·4PF_6 was different from that observed (Figure 7A) for the pseudorotaxanes *(SS)*-**29**/**1**·4PF_6 and *(RR)*-**29**/**1**·4PF_6.[36] One explanation for observing two maxima is an exciton coupling, implying that two chromophores—which are in a chiral geometry—are in each other's proximity. Another explanation for the observed phenomenon is that there are two different CT transitions in the **19**/**1**·4PF_6 [2]pseudorotaxane, one causing a positive and the other a negative Cotton effect. The superposition of both CD signals would then result in the observed CD spectrum. A third explanation is that **19** and **1**·4PF_6 self-assemble as more than one type of 1:1 complex or as aggregates of **19** and **1**·4PF_6. These different modes of complexation would then contribute to the observed CD effect. However, in the determination of the association constant for the 1:1 complex of **19** and **1**·4PF_6, no indications for such diverse behavior were found. In an additional experiment, CD effects were measured at two concentrations of **19**/**1**·4PF_6. For both concentrations, the same g_λ values were obtained, showing that the observed CD effect can be attributed solely to one type of [2]pseudorotaxane formed between **19** and **1**·4PF_6.

A series of temperature-dependent CD measurements on *(SS)*-**19**/**1**·4PF_6 and *(SS)*-**29**/**1**·4PF_6 revealed that, over the temperature range from −6 to +45 °C, the CD effects in both these pseudorotaxanes remained of the same type, implying that the different geometries observed for *(SS)*-**19**/**1**·4PF_6 and *(SS)*-**29**/**1**·4PF_6 could not be interconverted by temperature changes. These results confirm that *(SS)*-**19**/**1**·4PF_6 exists as one type of [2]pseudorotaxane. The g_{450} value for *(SS)*-**29**/**1**·4PF_6 is constant over the measured temperature domain, whereas the g_{440} value of *(SS)*-**19**/**1**·4PF_6 decreases with increasing temperature, suggesting a slight change in the geometry of this complex as a result of heating (Figure 8).

Finally, the CD spectra of the [2]pseudorotaxanes formed between *(SS)*-**34**−**37** and **1**·4PF_6 were recorded. Pseudorotaxanes *(SS)*-**36**/**1**·4PF_6 and *(SS)*-**37**/**1**·4PF_6 show a CD effect.[37] Remarkably, pseudorotaxanes *(SS)*-**34**/**1**·4PF_6 and *(SS)*-**35**/**1**·4PF_6 do *not* exhibit any CD activities. In *(SS)*-**34**/**1**·4PF_6, the positions of the chiral centers are the same as in the pseudorotaxanes described previously that exhibit CD activities. However, the second oxygen atoms in the polyether chains,

(33) For books on circular dichroism, see: (a) Nakanishi, K.; Berova, N.; Woody, R. W. *Circular Dichroism, Principles and Applications;* VCH Publishers: Inc.: New York, 1994. (b) Eliel, E. L.; Wilen, S. H. *Stereochemistry of Organic Compounds*; Wiley: New York, 1994. (c) Harada, N.; Nakanishi, K. *Circular Dichroic Spectroscopy, Exciton Coupling in Organic Stereochemistry;* Oxford University Press: Oxford, 1983.

(34) $g_\lambda = (\Delta\epsilon/\epsilon)_\lambda = (\Delta A/A)_\lambda = \psi_\lambda/(32980A_\lambda)$, with g_λ = dissymmetry factor measured at wavelength λ (in this paper mainly the values at the maxima of the CD spectra are reported), ψ_λ = measured CD effect in millidegrees at wavelength λ, A_λ = measured absorbance at wavelength λ, ϵ = specific absorbance, A = absorbance, $\Delta\epsilon = \epsilon_L - \epsilon_R$ = difference in specific absorbance between left and right circularly polarized light and $\Delta A = A_L - A_R$ = difference in absorbance between left and right circularly polarized light.

(35) These are low *g* values compared to *g* values of other types of electronic transitions. For example, n−π^*, $\pi-\pi^*$, $\pi-\pi^*$ couplet, $\pi_x-\pi_x^*$, $\pi_x-\pi_y^*$, and n−σ^* transitions have typical *g* values of 30×10^{-3}, 8×10^{-3}, 3×10^{-3}, 2×10^{-3}, and 1×10^{-3}, respectively. See ref 34b, p 1014. CD activity in charge-transfer transitions has also been observed in [2,2]-metacyclophanes. See: Knops, P.; Windscherf, P.-M.; Vögtle, F.; Roloff, A.; Jansen, M.; Nieger, M.; Niecke, E.; Okamoto, Y. *Chem. Ber.* **1991**, *124*, 1585−1590.

(36) The g_{440} values of the effects were approximately 4 times smaller than the g_{450} values observed for the **29**/**1**·4PF_6 pseudorotaxanes (9.4×10^{-5} and -8.3×10^{-5} for (*SS*)-**19** and (*RR*)-**19**, respectively).

(37) For both [2]pseudorotaxanes one maximum in the CD spectrum was observed, so a spectrum similar to that for *(SS)*-**29**/**1**·4PF_6 was obtained (see Figure 8A). For *(SS)*-**36**/**1**·4PF_6 and *(SS)*-**37**/**1**·4PF_6 *g* values of $g_{465} = -2.7 \times 10^{-4}$ and $g_{460} = -2.8 \times 10^{-4}$ were measured, respectively.

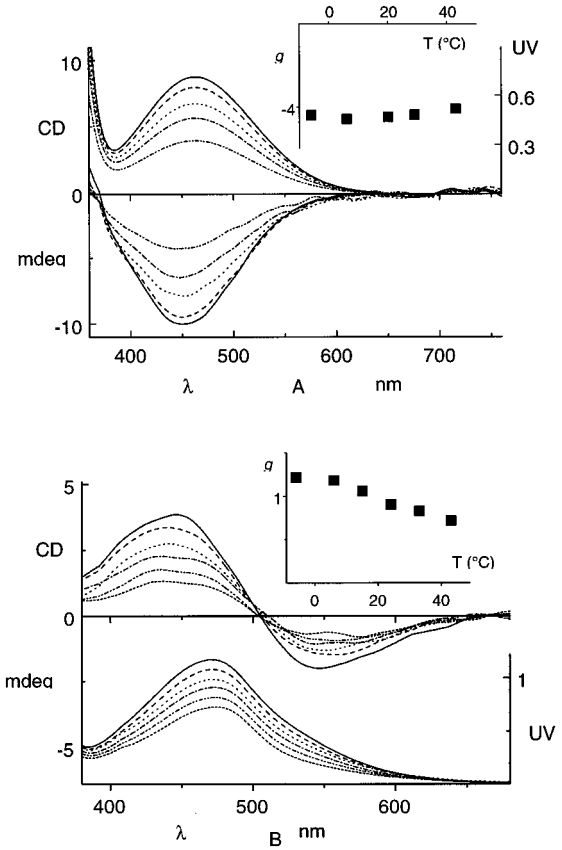

Figure 8. (a) CD and UV spectra for the pseudorotaxane *(SS)*-**29**/**1**·4PF_6 in MeCN at −6 °C (solid), 6 °C (dashed), 20 °C (dotted), 29 °C (dash−dot), and 43 °C (dash−dot−dot). The g_{450} $-T$ curve is also shown: g_{450} values ($\times 10^{-4}$) are depicted. (b) CD and UV spectra for pseudorotaxane *(SS)*-**19**/**1**·4PF_6 in MeCN at −6 °C (solid), 6 °C (dashed), 15 °C (dotted), 24 °C (dash−dot), 33 °C (dash−dot−dot), and 43 °C (short dash). The g_{440} $-T$ curve is also shown: g_{440} values ($\times 10^{-4}$) are depicted.

which could form hydrogen bonds to the acidic protons on **1**·4PF_6 and hence "lock" the pseudorotaxane in a chiral geometry, are "missing". It is difficult to explain the absence of CD activity in the CT band of the [2]pseudorotaxane *(SS)*-**35**/**1**·4PF_6. Apparently, even the subtle differences (only two methylene groups) between *(SS)*-**35**/**1**·4PF_6 and *(SS)*-**36**/**1**·4PF_6 result in the formation of different complexes in solution.

Conclusions

The introduction of constitutional asymmetry or chirality into noncentrosymmetric π-electron-rich guests bearing carboxylic acid termini leads to a number of geometries, both in solution and in the solid state. In the latter, the π-electron-rich guests are inserted into the π-electron-deficient cavity of $\mathbf{1}^{4+}$ with conformations that are dependent on the nature and configurations of the substituents present in their polyether backbones. Often, noncovalent bonding interactions between adjacent [2]-pseudorotaxanes bring about the formation of pseudopolyrotaxane structures. Also in solution, distinct differences between the [2]pseudorotaxane superstructures can be observed as evidenced by ^{1}H NMR and CD spectroscopies. In particular, it was found that subtle changes in the structures of the guests can direct the occurrence and the nature of the induced CD effect in the CT transition of the complex, showing that *different geometries of the [2]pseudorotaxanes are possible in solution. The [2]pseudorotaxanes which do show induced CD effects in the CT transitions prove that the chirality in the polyether chains of the π-electron rich polyether guests can be translated into a chiral geometry that becomes associated with the whole supramolecular structure.* It is proposed that, in solution, this chiral geometry is the result of the locking of the conformation of the guest as a result of hydrogen bonding between the oxygen atoms on it and the acidic α-bipyridinium protons on the tetracationic cyclophane. Thus, in solution, a variety of [2]-pseudorotaxanes differing in geometry are formed. Subtle changes in the structures of the π-electron-rich guests produce dramatic changes in the solution and solid-state structures of the resulting [2]pseudorotaxanes.

Experimental Section

General Methods. THF was distilled from sodium before use. Benzophenone was used as an indicator in this distillation procedure. Pyridine was distilled from KOH and stored on dried 3 Å molecular sieves. CH_2Cl_2 and TFA were both distilled from P_2O_5 before use. All other solvents and materials were used as received. The tetracationic cyclophane **1**·4PF_6,[20] the methyl ester **4**,[18] and the bistosylates **17** and **18**[20] were prepared using previously published procedures. Thin-layer chromatography (TLC) was performed on aluminum sheets (10 × 5 cm) coated with Merck 5735 Kieselgel 60F. Developed plates were air-dried, scrutinized under a UV lamp, and, if necessary, then sprayed with cerium(IV) sulfate−sulfuric acid reagent and heated to ca. 100 °C, sprayed with an aqueous KI/I_2 solution, or developed in an iodine tank. Kieselgel 60 (0.040−0.063 mm mesh, Merck 9385) or Merck flash silica gel 60 (particle size 0.040−0.063 mm) was used to perform column chromatography. Melting points were determined on an Electrothermal 9200 melting point apparatus or Büchi apparatus. Optical rotations were recorded on a JASCO DIP-370 polarimeter at a wavelength of 589 nm (sodium D-line). CD spectra were recorded on a JASCO J-600 spectropolarimeter. Mass spectra (MS) were obtained from either Kratos Profile or MS80RF instruments, the latter being equipped with a fast atom bombardment (FAB) facility (using a krypton primary atom beam in conjunction with a 3-nitrobenzyl alcohol matrix). FABMS were recorded in the positive-ion mode at a scan speed of 30 s per decade. Electrospray MS (ESMS) was performed on a Perkin-Elmer Sciex API-300 LC−MS/MS. GC/MS was performed on a HP 5790 GC with an OV-1 column and a HP 5970A MSD. ^{1}H NMR spectra were recorded on a Bruker AC300 (300 MHz), Bruker AM400 (400 MHz), or Bruker AMX400 (400 MHz) spectrometer (using the deuterated solvent as lock and residual solvent or tetramethylsilane as internal reference). ^{13}C NMR spectra were recorded on a Bruker AC300 (75 MHz), Bruker AM400 (100 MHz), or AMX 400 (100 MHz) spectrometer using a PENDANT pulse sequence (assuming $^1J_{CH} = 143$ Hz). Infrared spectra were taken on a Perkin-Elmer 1600 series FTIR spectrometer with wavenumbers between 4400 and 450 cm^{-1}. Microanalyses were performed by the University of North London Microanalytical Service and at the Laboratory of Organic Chemistry at Eindhoven University.

1-[2-(2-Methoxyethoxy)ethoxy]-4-(carboxymethoxy)benzene (5). The methyl ester **4**[18] (1.00 g, 3.5 mmol) was added to a solution of NaOH (430 mg, 10.6 mmol) in H_2O (100 mL), and the solution was heated under reflux for 4 h. After cooling to room temperature, acidification with dilute HCl (50 mL) gave the carboxylic acid **5** as a white crystalline solid (710 mg, 75%): mp 84−85 °C; EIMS *m/z* 270 $[M]^+$; ^{1}H NMR (CD_3CN, 300 MHz) δ 3.30 (3H, s), 3.50−3.47 (2H, m), 3.62−3.59 (2H, m), 3.75−3.72 (2H, m), 4.06−4.03 (2H, m), 4.59 (2H, s), 6.87 (4H, s), 9.50 (1H, br s); ^{13}C NMR (CD_3CN, 75 MHz) δ 58.9, 66.2, 69.0, 70.4, 71.1, 72.6, 116.5, 116.5, 153.1, 154.7, 170.6. Anal. Calcd for $C_{13}H_{18}O_6$ (270): C, 43.81; H, 6.42. Found: C, 43.66; H, 6.31.

4-Methyl-2*(S)*-[(tetrahydropyran-2-yl)oxy]pentan-1-ol [*(S)*-14]. Commercially available *(S)*-leucine [*(S)*-**6**] (ee > 97%, as measured on a chiral Daicell CR (+) HPLC column) was transformed into *(S)*-leucic acid [*(S)*-**8**] by diazotization with $NaNO_2$ and H_2SO_4 in H_2O. Esterification in EtOH/PhMe containing a few drops of concentrated HCl yielded ethyl *(S)*-leucate [*(S)*-**10**] (ee > 97% as determined on a permethylated β-cyclodextrin capillary GC column; i.e., no significant

racemization had occurred during the reaction sequence). Protection with DHP gave compound *(S)*-**12**, and subsequent reduction afforded the protected alcohol *(S)*-**14**. All spectroscopic data of the various compounds were in agreement with the data already reported in the literature by Mori et al.[19c]

2-*(S)*-[(Tetrahydropyran-2-yl)oxy]propan-1-ol 4-Methylbenzenesulfonate [*(S)*-15] and *(R)*-15. The synthesis of compound *(S)*-**15** was carried out starting from commercially available ethyl *(S)*-lactate [*(S)*-**9**]. GC analysis with a permethylated β-cyclodextrin capillary column showed *(S)*-**9** to have an ee > 99.5% ($[\alpha]^{24}_D = -13.6°$ ($c = 3.25$ in MeCN)). Reaction of *(S)*-**9** with DHP in Et_2O and a catalytic amount of *p*-toluenesulfonic acid yielded *(S)*-**11**. Reduction of the ester function yielded compound *(S)*-**13**. All spectroscopic data of the various compounds were in agreement with the data already reported in the literature by Perkins.[19a] Tosylation of *(S)*-**13** with *p*-toluenesulfonyl chloride in C_5H_5N afforded *(S)*-**15** which was used in subsequent reactions without further purification. The synthesis of compound *(R)*-**15** was carried out starting from *(RR)*-lactide *(RR)*-**7**. Transesterification of this lactide in a refluxing mixture of EtOH, PhMe, and a few drops of concentrated HCl and subsequent distillation afforded ethyl *(R)*-lactate [*(R)*-**9**] in a 76% yield. GC analysis on a permethylated β-cyclodextrin capillary column showed *(R)*-**9** to have an ee > 99.9% ($[\alpha]^{24}_D = +13.4°$ ($c = 3.19$ in MeCN)). Ethyl *(R)*-lactate [*(R)*-**9**] was converted into *(R)*-**15** employing the same procedure as that described for *(S)*-**9**.

1,4-Bis[2*(S)*-hydroxypropoxy]benzene [*(SS)*-19] and *(RR)*-19. A solution of compound *(S)*-**15** (9.4 g, 29.9 mmol) in THF (15 mL) was added dropwise to a refluxing suspension of hydroquinone **16** (1.5 g, 13.6 mmol) and KOH (1.65 g, 29.5 mmol) in EtOH (15 mL). The solution was maintained at reflux for 2 days. After removal of the solvents in vacuo, a 1 M NaOH aqueous solution was added and the mixture was extracted with CH_2Cl_2. The collected organic layers were washed with a 1 M NaOH aqueous solution and dried with $MgSO_4$. The crude material was dissolved in MeOH, and a catalytic amount of *p*-toluenesulfonic acid was added. Overnight stirring at room temperature resulted in deprotection of the THP group. The reaction was quenched by addition of $NaHCO_3$, and the solvent was removed in vacuo. The reaction mixture was purified by column chromatography (SiO_2, hexane/EtOAc (3:5) ($R_f = 0.25$)), and crystallization from hexane/PhMe (1:1) to give *(SS)*-**19** as a white solid (1.0 g, 32%): mp 95 °C; $[\alpha]^{25}_D = +5.8°$ ($c = 2.1$ in MeCN); ^{1}H NMR ($CDCl_3$, 400 MHz) δ 6.85 (4H, s), 4.15 (2H, m), 3.9 (2H, dd, $^2J = 9.2$ Hz, $^3J = 3.1$ Hz), 3.75 (2H, dd, $^2J = 9.2$ Hz, $^3J = 7.9$ Hz), 2.65 (2H, br s), 1.25 (6H, d, $^3J = 6.4$ Hz); ^{13}C NMR ($CDCl_3$, 100 MHz) δ 153.0, 115.5, 74.0, 66.2, 18.7; FTIR (KBr, cm^{-1}) $\nu = 3328$, 2976, 2917, 2868, 1514, 1459, 1383, 1290, 1245, 1111, 1053, 994, 959, 819, 788, 520. Anal. Calcd for $C_{12}H_{18}O_4$ (226.272): C, 63.70; H, 8.02. Found: C, 63.50; H, 7.90.

(RR)-**19** was similarly prepared from compound *(R)*-**15** and hydroquinone to afford *(RR)*-**19** as a white solid (23%): mp 96 °C; $[\alpha]^{23}_D = -9.0°$ ($c = 1.9$ in MeCN). The spectroscopic data for compound *(RR)*-**19** were identical with those reported for compound *(SS)*-**19**. Anal. Calcd for $C_{12}H_{18}O_4$ (226.272): C, 63.70; H, 8.02. Found: C, 63.88; H, 8.21.

1,4-Bis[2-(2*(S)*-hydroxypropoxy)ethoxy]benzene [*(SS)*-20] and *(RR)*-20. 2*(S)*-[(Tetrahydropyran-2-yl)oxy]propan-1-ol [*(S)*-**13**] (3.3 g, 20.3 mmol, 2.3 mol equiv), the bistosylate **17** (4.4 g, 8.7 mmol), and KOH (4.5 g, 80.4 mmol) were suspended in dry THF (50 mL). The suspension was maintained at reflux for 60 h under an argon atmosphere. The solvent was then removed in vacuo, H_2O was added, and the residue was extracted with CH_2Cl_2. The combined organic layers were washed with H_2O and concentrated in vacuo. The crude material was dissolved in MeOH, and a catalytic amount of *p*-toluenesulfonic acid was added. Stirring at room temperature for 1 h was sufficient to deprotect the THP group. The reaction was quenched with $NaHCO_3$, and the solvent was then removed in vacuo, H_2O was added and the residue was extracted with CH_2Cl_2 to give 2.8 g of a crude product, which was purified by flash column chromatography (SiO_2, hexane/THF (4:3) ($R_f = 0.15$)), followed by crystallization from PhMe to yield *(SS)*-**20** as a white solid (1.35 g, 49%): mp 67−68 °C; $[\alpha]^{26}_D = +12.2°$ ($c = 0.89$ in MeCN); ^{1}H NMR ($CDCl_3$, 400 MHz) δ 6.85 (4H, s), 4.10 (4H, m), 4.00 (2H, m), 3.85 (4H, m), 3.55 (2H, dd, $^2J = 9.8$ Hz, $^3J = 3.1$ Hz), 3.30 (2H, dd, $^2J = 9.8$ Hz, $^3J = 8.2$ Hz), 2.70 (2H, br s), 1.10 (6H, d, $^3J = 6.6$ Hz); ^{13}C NMR ($CDCl_3$, 100 MHz) δ 152.8, 115.4, 76.8, 69.6, 67.7, 66.0, 18.4; FTIR (KBr, cm^{-1}) $\nu = 3483$, 2970, 2907, 1513, 1454, 1371, 1328, 1279, 1232, 1135, 1043, 929, 891, 824, 751; GC/MS peak at *m/z* 314.05 (12.1% abundance relative to 59.00).

In an analogous fashion, *(RR)*-**20** was synthesized from *(R)*-**13** and bistosylate **17**. The alcohol *(RR)*-**20** was isolated as a white solid in 51% yield: $[\alpha]^{21}_D = -13.4°$ ($c = 1.13$ in MeCN). All spectroscopic data were identical with those reported for compound *(SS)*-**20**. Anal. Calcd for $C_{16}H_{26}O_6$ (314.173): C, 61.11; H, 8.34. Found: C, 61.44; H, 8.04.

1,4-Bis[2-(2-(2*(S)*-hydroxypropoxy)ethoxy)ethoxy]benzene [*(SS)*-21] and *(RR)*-21. These compounds were prepared from bisotosylate **18** and alcohol (*S*)-**13** or (*R*)-**13**, by a procedure similar to that reported for (*SS*)-**20** and (*RR*)-**20**. The compounds were purified by flash column chromatography (SiO_2, hexane/THF (2:3) ($R_f = 0.20$)) to yield (*SS*)-**21** as a white solid (72%) and (*RR*)-**21** as a clear, oily product (45%) which slowly solidified (mp 33 °C). Spectral data (for both compounds): ^{1}H NMR ($CDCl_3$, 400 MHz) δ 6.80 (4H, s), 4.10 (4H, m), 3.95 (2H, m), 3.80 (4H, m), 3.70 (8H, m), 3.50 (2H, dd, $^2J = 9.9$ Hz, $^3J = 2.9$ Hz), 3.25 (2H, dd, $^2J = 9.9$ Hz, $^3J = 8.4$ Hz), 2.80 (2H, br s), 1.10 (6H, d, $^3J = 6.2$ Hz); ^{13}C NMR ($CDCl_3$, 100 MHz) δ 153.0, 115.6, 76.9, 70.6, 70.5, 69.8, 68.0, 66.2, 18.4; FTIR (KBr, cm^{-1}) $\nu = 3423$, 2970, 2907, 1508, 1458, 1232, 1110, 935, 830. Data on (*SS*)-**21**: mp = 32−34 °C; $[\alpha]^{26}_D = 9.4°$ ($c = 0.87$ in MeCN). Anal. Calcd for $C_{20}H_{34}O_8$ (402.225): C, 59.67; H, 8.52. Found: C, 59.39; H, 8.85. Data on (*RR*)-**21**: $[\alpha]^{21}_D = -11.7°$ ($c = 0.84$ in MeCN); GC/MS peaks at *m/z* 401.95 and 402.92 (12.1% and 2.9% abundance relative to 58.95).

1,4-Bis[2-(2*(S)*-hydroxy-4-methylpentoxy)ethoxy]benzene [*(SS)*-22]. This compound was prepared from bistosylate **17** and alcohol (*S*)-**14** by a procedure similar to that reported for (*SS*)-**20**. The product was purified by flash column chromatography (SiO_2, hexane/EtOAc (1:1) ($R_f = 0.27$)) to yield (*SS*)-**22** as a white solid (32%): mp 36−38 °C; $[\alpha]^{26}_D = -3.7°$ ($c = 5.09$ in MeCN); ^{1}H NMR ($CDCl_3$, 400 MHz) δ 6.85 (4H, s), 4.05 (4H, m), 3.90 (2H, m), 3.80 (4H, m), 3.55 (2H, dd, $^2J = 9.6$ Hz, $^3J = 2.8$ Hz), 3.30 (2H, dd, $^2J = 9.6$ Hz, $^3J = 8.0$ Hz), 2.50 (2H, br s), 1.80 (2H, m), 1.40 (2H, ddd, $^2J = 13.9$ Hz, $^3J = 9.0$ Hz, $^3J = 5.5$ Hz), 1.15 (2H, ddd, $^2J = 13.9$ Hz, $^3J = 8.4$ Hz, $^3J = 4.1$ Hz), 0.93 (6H, d, $^3J = 6.6$ Hz), 0.90 (6H, d, $^3J = 6.6$ Hz); ^{13}C NMR ($CDCl_3$, 100 MHz) δ 153.0, 115.6, 76.3, 69.9, 68.3, 68.0, 41.8, 24.4, 23.4, 22.0; FTIR (KBr, cm^{-1}) $\nu = 3442$, 2955, 1510, 1455, 1367, 1286, 1231, 1128, 1064, 930, 826, 757. Anal. Calcd for $C_{22}H_{38}O_6$ (398.267): C, 66.29; H, 9.62. Found: C, 66.59; H, 9.47.

1,4-Bis[2-(2-(2*(S)*-hydroxy-4-methylpentoxy)ethoxy)ethoxy]benzene [*(SS)*-23]. This compound was prepared from bistosylate **18** and alcohol (*S*)-**14** by a procedure similar to that reported for (*SS*)-**20**. The product was purified by flash column chromatography (SiO_2, hexane/EtOAc (2:3) ($R_f = 0.16$)) to yield (*SS*)-**23** as a clear oil (38%): $[\alpha]^{26}_D = -2.7°$ ($c = 4.76$ in MeCN); ^{1}H NMR ($CDCl_3$, 400 MHz) δ 6.85 (4H, s), 4.05 (4H, m), 3.90 (2H, m), 3.80 (4H, m), 3.70 (8H, m), 3.50 (2H, dd, $^2J = 9.9$ Hz, $^3J = 3.0$ Hz), 3.25 (2H, dd, $^2J = 9.9$ Hz, $^3J = 8.3$ Hz), 2.65 (2H, br s), 1.80 (2H, m), 1.40 (2H, ddd, $^2J = 13.6$ Hz, $^3J = 8.8$ Hz, $^3J = 5.0$ Hz), 1.10 (2H, ddd, $^2J = 13.6$ Hz, $^3J = 8.8$ Hz, $^3J = 4.4$ Hz), 0.92 (6H, d, $^3J = 6.6$ Hz), 0.89 (6H, d, $^3J = 6.7$ Hz); ^{13}C NMR ($CDCl_3$, 100 MHz) δ 153.0, 115.5, 76.2, 70.7, 70.5, 69.8, 68.3, 68.0, 41.8, 24.4, 23.4, 22.0; FTIR (KBr, cm^{-1}) $\nu = 3440$, 2955, 1510, 1455, 1367, 1285, 1232, 1112, 1065, 950, 828. Anal. Calcd for $C_{26}H_{46}O_8$ (486.319): C, 64.16; H, 9.53. Found: C, 64.42; H, 9.69.

1,4-Bis[2*(S)*-(*tert*-butoxycarbonylmethoxy)propoxy]benzene [*(SS)*-24] and *(RR)*-24. The diol *(SS)*-**19** (0.31 g, 1.37 mmol) and *t*-BuOK (0.34 g, 3.04 mmol, 2.2 mol equiv) were dissolved in *t*-BuOH (4 mL) at 30−40 °C. After the mixture had been allowed to cool to room temperature, *tert*-butyl bromoacetate (1.04 g, 5.3 mmol, 3.9 mol equiv) was added dropwise while the solution was cooled in a water bath. A precipitate formed immediately. The suspension was stirred overnight, after which the reaction was quenched with an aqueous $NaHCO_3$ solution. The solvent was removed in vacuo, and H_2O was added to the semisolid material. Subsequent extraction with CH_2Cl_2 and

concentration of the organic layers gave the crude product that was purified by flash column chromatography (SiO_2, hexane/EtOAc (85:15) ($R_f = 0.20$)) to yield *(SS)*-**24** as a clear oil (270 mg, 45%): $[\alpha]^{27}_D = -40.3°$ ($c = 7.96$ in Me_2CO); ^{1}H NMR ($CDCl_3$, 400 MHz) δ 6.85 (4H, s), 4.15 (2H, d, $^2J = 16.5$ Hz), 4.10 (2H, d, $^2J = 16.5$ Hz), 4.0 (2H, dd, $^2J = 9.2$ Hz, $^3J = 5.5$ Hz), 3.85 (4H, m), 1.45 (18H, s), 1.30 (6H, d, $^3J = 6.2$ Hz); ^{13}C NMR ($CDCl_3$, 100 MHz) δ 169.8, 152.8, 115.2, 81.2, 74.6, 72.4, 67.4, 27.9, 17.1; FTIR (KBr, cm^{-1}) $\nu = 2977$, 2932, 1748, 1508, 1456, 1368, 1228, 1127, 1045, 939, 826. Anal. Calcd for $C_{24}H_{38}O_8$ (454.56): C, 63.42; H, 8.43. Found: C, 63.68; H, 8.87.

(RR)-**24** was synthesized in the same way from diol *(RR)*-**19** and *tert*-butyl bromoacetate to afford a clear oil in 46% yield: $[\alpha]^{27}_D = +44.1°$ ($c = 6.97$ in Me_2CO). All spectroscopic data were identical with those reported for (*SS*)-**24**. Anal. Calcd. for $C_{24}H_{38}O_8$ (454.56): C, 63.42; H, 8.43. Found: C, 63.32; H, 8.43.

1,4-Bis[2-(2(*S*)-(*tert*-butoxycarbonylmethoxy)propoxy)ethoxy]-benzene [*(SS)*-25] and (*RR*)-25. These compounds were prepared by procedures similar to those reported for (*SS*)-**24** and (*RR*)-**24**. The products were purified by flash column chromatography (SiO_2, hexane/EtOAc (5:2) ($R_f = 0.12$)) to yield clear oils (46% and 36% yields for (*SS*)-**25** and (*RR*)-**25**, respectively). Spectral data (for both compounds): ^{1}H NMR ($CDCl_3$, 400 MHz) δ 6.85 (4H, s), 4.15 (2H, d, $^2J = 15.5$ Hz), 4.10 (2H, d, $^2J = 15.5$ Hz), 4.05 (4H, m), 3.80 (4H, m), 3.75 (2H, m), 3.60 (2H, dd, $^2J = 10.1$ Hz, $^3J = 6.4$ Hz), 3.55 (2H, dd, $^2J = 10.1$ Hz, $^3J = 4.2$ Hz),1.45 (18H, s), 1.20 (6H, d, $^3J = 6.7$ Hz); ^{13}C NMR ($CDCl_3$, 100 MHz) δ 170.1, 153.1, 115.5, 81.2, 75.7, 75.2, 69.9, 68.0, 67.4, 28.0, 17.0; FTIR (KBr, cm^{-1}) $\nu = 2977$, 2932, 1747, 1505, 1454, 1369, 1290, 1233, 1132, 1065, 938, 827, 751. Data on (*SS*)-**25**: $[\alpha]^{29}_D = -5.8°$ ($c = 3.28$ in MeCN). Anal. Calcd for $C_{28}H_{46}O_{10}$ (542.309): C, 61.96; H, 8.55. Found: C, 62.39; H, 8.43. Data on (*RR*)-**25**: $[\alpha]^{26}_D = +5.9°$ ($c = 1.19$ in MeCN). Anal. Calcd for $C_{28}H_{46}O_{10}$ (542.309): C, 61.96; H, 8.55. Found: C, 62.03; H, 8.57.

1,4-Bis[2-(2-(2*(S)*-(*tert*-butoxycarbonylmethoxy)propoxy)ethoxy)-ethoxy]benzene [(*SS*)-26] and (*RR*)-26. These compounds were prepared by procedures similar to those reported for (*SS*)-**24** and (*RR*)-**24**. The products were purified by flash column chromatography (SiO_2, hexane/EtOAc (3:2) ($R_f = 0.10$)) to yield clear oils (38% and 44% yields for *(SS)*-**26** and (*RR*)-**26**, respectively). Spectral data (for both compounds): ^{1}H NMR ($CDCl_3$, 400 MHz) δ 6.80 (4H, s), 4.10 (2H, d, $^2J = 16.5$ Hz), 4.05 (6H, m), 3.85 (4H, m), 3.75−3.60 (10H, m), 3.55 (2H, dd, $^2J = 10.3$ Hz, $^3J = 6.3$ Hz), 3.45 (2H, dd, $^2J = 10.3$ Hz, $^3J = 4.0$ Hz), 1.45 (18H, s), 1.20 (6H, d, $^3J = 6.2$ Hz); ^{13}C NMR ($CDCl_3$, 100 MHz) δ 170.1, 153.0, 115.5, 81.2, 75.5, 75.2, 70.8, 70.7, 69.8, 68.0, 67.4, 28.1, 17.1; FTIR (KBr, cm^{-1}) $\nu = 2975$, 2931, 1748, 1510, 1455, 1368, 1290, 1230, 1125, 1065, 941, 827, 752. Data on (*SS*)-**26**: $[\alpha]^{26}_D = -4.0°$ ($c = 3.37$ in MeCN). Anal. Calcd for $C_{32}H_{54}O_{12}$ (630.361): C, 60.92; H, 8.63. Found: C, 60.48; H, 8.71. Data on (*RR*)-**26**: $[\alpha]^{26}_D = +3.7°$ ($c = 2.42$ in MeCN). Anal. Calcd for $C_{32}H_{54}O_{12}$ (630.361): C, 60.92; H, 8.63. Found: C, 60.66; H, 8.89.

1,4-Bis[2-(2*(S)*-(*tert*-butoxycarbonylmethoxy)4-methylpentoxy)-ethoxy]benzene [*(SS)*-27]. This compound was prepared by a procedure similar to that described for (*SS*)-**24**. The product was purified by flash column chromatography (SiO_2, hexane/EtOAc (3:1) ($R_f = 0.23$)) to yield a clear oil (38%). $[\alpha]^{25}_D = -14.6°$ ($c = 2.22$ in MeCN); ^{1}H NMR ($CDCl_3$, 400 MHz) δ 6.85 (4H, s), 4.20 (2H, d, $^2J = 16.5$ Hz), 4.10 (2H, d, $^2J = 16.5$ Hz), 4.05 (4H, m), 3.80 (4H, m), 3.60−3.50 (6H, m), 1.80 (2H, m), 1.50 (20H, m), 1.25 (2H, m), 0.92 (6H, d, $^3J = 6.6$ Hz), 0.90 (6H, d, $^3J = 6.6$ Hz); ^{13}C NMR ($CDCl_3$, 100 MHz) δ 170.0, 153.1, 115.5, 81.1, 77.8, 75.1, 69.9, 68.3, 68.0, 40.9, 28.1, 24.3, 23.1, 22.4; FTIR (KBr, cm^{-1}) $\nu = 2956$, 2870, 1748, 1509, 1455, 1392, 1368, 1301, 1231, 1128, 1047, 929, 826, 751. Anal. Calcd for $C_{34}H_{58}O_{10}$ (626.403): C, 65.13; H, 9.33. Found: C, 65.67; H, 9.57.

1,4-Bis[2-(2-(2*(S)*-(*tert*-butoxycarbonylmethoxy)-4-methylpentoxy)-ethoxy)ethoxy]benzene [*(SS)*-28]. This compound was prepared by a procedure similar to that described for (*SS*)-**24**. The product was purified by flash column chromatography (SiO_2, hexane/EtOAc (2:1) ($R_f = 0.21$)) to yield a clear oil (31%): $[\alpha]^{25}_D = -18.6°$ ($c = 1.56$ in MeCN); ^{1}H NMR ($CDCl_3$, 400 MHz) δ 6.85 (4H, s), 4.15 (2H, d, $^2J = 16.2$ Hz), 4.10 (2H, d, $^2J = 16.2$ Hz), 4.05 (4H, m), 3.85 (4H, m), 3.70 (4H, m), 3.65 (6H, m), 3.55 (4H, m), 1.85 (2H, m), 1.45 (20H, m), 1.25 (2H, m), 0.92 (6H, d, $^3J = 2.5$ Hz), 0.90 (6H, d, $^3J = 2.6$ Hz); ^{13}C NMR ($CDCl_3$, 100 MHz) δ 170.0, 153.0, 115.5, 81.1, 77.8, 74.9, 70.7 (2), 69.8, 68.2, 68.0, 41.0, 28.1, 24.3, 23.1, 22.4; FTIR (KBr, cm^{-1}) $\nu = 2955$, 2869, 1750, 1508, 1455, 1392, 1368, 1300, 1230, 1127, 1068, 941, 826, 751. Anal. Calcd for $C_{38}H_{66}O_{12}$ (714.455): C, 63.82; H, 9.31. Found: C, 63.57; H, 9.30.

1,4-Bis[2*(S)*-(carboxymethoxy)propoxy]benzene [*(SS)*-29] and (*RR*)-29. The diester *(SS)*-**24** (170 mg, 0.37 mmol) was stirred overnight in dry CH_2Cl_2 (5 mL) in the presence of TFA (0.4 mL). The solvent was removed in vacuo to afford *(SS)*-**29** as a sticky oily product in quantitative yield: $[\alpha]^{22}_D = -31.3°$ ($c = 4.35$ in Me_2CO); ^{1}H NMR ($CDCl_3$, 400 MHz) δ 11.1 (2H, br s), 6.80 (4H, s), 4.35 (2H, d, $^2J = 17.2$ Hz), 4.20 (2H, d, $^2J = 17.2$ Hz), 3.90 (6H, m), 1.25 (6H, d, $^3J = 6.3$ Hz); ^{13}C NMR ($CDCl_3$, 100 MHz) δ 174.9, 152.5, 115.3, 75.9, 72.3, 66.9, 16.7; ESMS *m*/*z* 341 $[M - H]^-$.

(RR)-**29** was prepared from *(RR)*-**24** in a similar way. A sticky oily product in quantitative yield was obtained: $[\alpha]^{21}_D = +32.5°$ ($c = 6.80$ in Me_2CO). The spectroscopic data were identical with those reported for compound (*SS*)-**29**: ESMS *m*/*z* 341 $[M - H]^-$.

1,4-Bis[2-(2*(S)*-(carboxymethoxy)propoxy)ethoxy]benzene [*(SS)*-30] and (*RR*)-30. The diester *(SS)*-**25** (160 mg, 0.30 mmol) was stirred in an HBr solution of dry CH_2Cl_2 for 1 h at 0 °C. The solvent was removed in vacuo to yield *(SS)*-**30** as a sticky, oily compound (130 mg, 100%). TLC and NMR spectroscopy indicated that the purity of the product was better than 95%: $[\alpha]^{24}_D = +5.8°$ ($c = 3.12$ MeCN/Me_2CO (2/3, v/v)); ^{1}H NMR ($CDCl_3$, 400 MHz) δ 10.7 (2H, br s), 6.85 (4H, s), 4.25 (2H, d, $^2J = 17.3$ Hz), 4.10 (2H, d, $^2J = 17.3$ Hz), 4.05 (4H, m), 3.85 (4H, m), 3.70 (2H, m), 3.55 (4H, m), 1.15 (6H, d, $^3J = 6.3$ Hz); ^{13}C NMR ($CDCl_3$, 100 MHz) δ 173.3, 152.9, 115.6, 76.8, 75.0, 69.9, 67.6, 67.0, 16.3; FTIR (KBr, cm^{-1}) $\nu = 3100$, 2930, 1788, 1766, 1732, 1510, 1455, 1367, 1220, 1170, 1130, 928, 827, 756; ESMS *m*/*z* 429.0 $[M - H]^-$.

(RR)-**30** was prepared from *(RR)*-**25** in a similar deprotection procedure to yield a sticky oil in quantitative yield. TLC and NMR spectroscopy indicated that the purity of the product was better than 95%: $[\alpha]_D^{20} = -7.4°$ ($c = 2.54$ in MeCN/Me_2CO (2:3 v/v)). The spectroscopic data were identical with those reported for compound (*SS*)-**30**: ESMS *m*/*z* 429 $[M - H]^-$.

1,4-Bis[2-(2-(2(S)-(carboxymethoxy)propoxy)ethoxy)-ethoxy]benzene [*(SS)*-31] and (*RR*)-31. The diester *(SS)*-**26** (155 mg, 0.25 mmol) was stirred in an HBr solution of dry CH_2Cl_2 for 1.5 h at 0 °C. The solvent was removed in vacuo to yield *(SS)*-**31** as a clear oil (130 mg, 100%). TLC and NMR spectroscopy indicated that the purity of the product was better than 95%: $[\alpha]^{21}_D = +16.5°$ ($c = 2.60$ in MeCN); ^{1}H NMR ($CDCl_3$, 400 MHz) δ 10.0 (2H, br s), 6.80 (4H, s), 4.25 (2H, d, $^2J = 17.3$ Hz), 4.10 (6H, m), 3.85 (4H, m), 3.70 (10H, m), 3.50 (4H, m), 1.15 (6H, d, $^3J = 6.2$ Hz); ^{13}C NMR ($CDCl_3$, 100 MHz) δ 173.0, 152.8, 115.4, 76.7, 74.7, 70.5, 70.2, 69.7, 67.8, 66.9, 16.1; FTIR (KBr, cm^{-1}) $\nu = 3200$, 2920, 1766, 1760, 1505, 1455, 1355, 1230, 1120, 1065, 930, 830, 755; ESMS *m*/*z* 517.2 $[M - H]^-$.

(RR)-**31** was prepared by stirring the diester *(RR)*-**26** in TFA for 1 h at room temperature. The solvent was removed in vacuo to yield (*RR*)-**31** as a brown, clear oil (100%). TLC and NMR spectroscopy indicated that the purity of the product was better than 95%: $[\alpha]^{20}_D = -9.5°$ ($c = 3.90$ in MeCN/Me_2CO (2:3 v/v)). The spectroscopic data were identical with those reported for compound (*SS*)-**31**: ESMS *m*/*z* 517.1 $[M - H]^-$.

1,4-Bis[2-(2*(S)*-(carboxymethoxy)-4-methylpentoxy)ethoxy]benzene [*(SS)*-32]. The diester *(SS)*-**27** (110 mg, 0.18 mmol) was stirred in an HBr solution of dry CH_2Cl_2 for 1.5 h at 0 °C. The solvent was removed in vacuo to yield *(SS)*-**32** as a clear oil (90 mg, 100%). TLC and NMR spectroscopy indicated that the purity of the product was better than 95%: $[\alpha]^{21}_D = +1.1°$ ($c = 4.4$ in MeCN); ^{1}H NMR ($CDCl_3$, 400 MHz) δ 10.0 (2H, br s), 6.8 (4H, s), 4.30 (2H, d, $^2J = 17.3$ Hz), 4.15 (2H, d, $^2J = 17.3$ Hz), 4.05 (4H, m), 3.85 (4H, m), 3.70−3.50 (6H, m), 1.70 (2H, m), 1.50 (2H, m), 1.25 (2H, m), 0.90 (12H, d, $^3J = 6.6$ Hz); ^{13}C NMR ($CDCl_3$, 100 MHz) δ 173.3, 152.9, 115.7, 79.5, 74.5, 70.0, 68.1, 67.6, 40.6, 24.4, 23.0, 22.4; FTIR (KBr, cm^{-1}) $\nu = 3174$, 2956, 1766, 1732, 1505, 1455, 1368, 1283, 1231, 1130, 928, 827, 757; ESMS *m*/*z* 512.9 $[M - H]^-$.

Table 3. Crystal Data, Data Collection and Refinement Parameters[a]

data	**5**	**5/1**·4PF_6	*(SS)*-**30/1**·4PF_6	*(SS)*-**37/1**·4PF_6
formula	$C_{13}H_{18}O_6$	$C_{49}H_{50}N_4O_6$·4PF6	$C_{56}H_{62}N_4O_{10}$·4PF6	$C_{54}H_{62}N_4O_6$·4PF6
solvent		5MeCN	2MeCN	2.5MeCN
formula weight	270.3	1576.1	1613.1	1545.6
color, habit	clear block	orange plate	red rhombs	red blocks
crystal size / mm	0.87 × 0.51 × 0.33	0.50 × 0.50 × 0.17	0.83 × 0.40 × 0.40	0.67 × 0.60 × 0.53
lattice type	triclinic	triclinic	monoclinic	triclinic
space group	*P*T	*P*T	$P2_1$	*P*1
cell dimensions: *a*/Å	7.735(1)	13.322(4)	11.554(2)	11.382(1)
b/Å	11.868(3)	15.097(3)	18.325(4)	12.742(1)
c/Å	15.122(4)	18.748(4)	17.823(5)	13.863(1)
α/deg	95.72(2)	95.99(2)		86.01(1)
β/deg	94.58(2)	105.11(2)	100.86(2)	75.21(1)
γ/deg	95.44(2)	101.73(2)		64.65(1)
V/Å^3	1369.4(5)	3515(2)	3706(1)	1754.9(2)
Z	4[b]	2	2	1
D_c/(g cm^{-3})	1.311	1.489	1.446	1.463
F(000)	576	1612	1652	793
μ/mm^{-1}	0.88	2.06	2.00	2.04
θ range/deg	3.0−62.0	2.5−63.0	2.5−62.1	5.0−60.0
no. of unique reflections				
measured	4299	10291	6039	5413
observed, $\|F_o\| > 4\sigma(\|F_o\|)$	3922	8364	4092	4918
no. of variables	344	1012	628	896
R_1[c]	0.054	0.071	0.131	0.064
wR_2[d]	0.153	0.184	0.377	0.163
weighting factors *a*, *b*[e]	0.081, 0.576	0.104, 5.011	0.306, 3.939	0.096, 2.579
largest difference peak, hole/eÅ^{-3}	0.39, −0.39	0.80, −0.67	0.87, −0.50	0.53, −0.45

[a] Details in common: graphite-monochromated Cu Kα radiation, ω scans, Siemens P4 diffractometer, 293 K, refinement based on *F*.[2] [b] There are two crystallographically independent molecules in the asymmetric unit. [c] $R_1 = \Sigma||F_o| - |F_c||/\Sigma|F_o|$. [d] $wR_2 = \{\Sigma w(F_o^2 - F_c^2)^2/\Sigma w(F_o^2)^2\}^{1/2}$. [e] $w^{-1} = \sigma^2(F_o^2) + (aP)^2 + bP$.

1,4-Bis[2-(2-(2*(S)*-(carboxymethoxy)-4-methylpentoxy)ethoxy)-ethoxy]benzene [*(SS)*-33]. The diester *(SS)*-**28** (155 mg, 0.25 mmol) was stirred in an HBr solution of dry CH_2Cl_2 for 1.5 h at 0 °C. The solvent was removed in vacuo to yield *(SS)*-**33** as a clear oil (130 mg, 100%). TLC and NMR spectroscopy indicated that the purity of the product was better than 95%: $[\alpha]^{25}_D = +5.4°$ (*c* = 1.17 in MeCN); ^{1}H NMR ($CDCl_3$, 400 MHz) δ 9.8 (2H, br s), 6.8 (4H, s), 4.25 (2H, d, ^2J = 17.3 Hz), 4.05 (2H, d, ^2J = 17.3 Hz), 4.00 (4H, m), 3.80 (4H, m), 3.70 (8H, m), 3.65−3.45 (6H, m), 1.70 (2H, m), 1.45 (2H, m), 1.25 (2H, ddd, ^2J = 14.0 Hz, ^3J = 7.5 Hz, ^3J = 5.7 Hz), 0.90 (12H, d, ^3J = 6.6 Hz); ^{13}C NMR ($CDCl_3$, 100 MHz) δ 173.0, 152.8, 115.4, 79.4, 74.1, 70.5, 70.2, 69.7, 68.0, 67.8, 40.5, 24.2, 22.9, 22.4; ESMS *m*/*z* 601.4 $[M - H]^-$.

1,4-Bis(2*(S)*-methylbutoxy)benzene [(*SS*)-34]. Hydroquinone **16** (305 mg, 2.77 mmol), KOH (360 mg, 6.43 mmol), and a catalytic amount of tetrabutylammonium iodide were suspended in EtOH (5 mL). The suspension turned brown. The tosylate of 2*(S)*-methylbutanol[21] (1.5 g, 6.20 mmol) in dry THF (10 mL) was added dropwise, after which the suspension was brought to reflux for 48 h. The reaction mixture was poured into a mixture of CH_2Cl_2 and a 1 M NaOH aqueous solution. The aqueous layer was extracted with CH_2Cl_2. The combined organic layers were dried ($MgSO_4$), filtered, and concentrated in vacuo to give 0.90 g of crude material, which was purified by flash column chromatography (SiO_2, hexane/CH_2Cl_2, (7:3)) to yield *(SS)*-**34** as a white solid (415 mg, 60%): mp 27−29 °C; $[\alpha]^{28}_D = +15.1°$ (*c* = 2.1 in $CHCl_3$); ^{1}H NMR ($CDCl_3$, 400 MHz) δ 6.85 (4H, s), 3.75 (2H, dd, ^2J = 8.9 Hz, ^3J = 5.8 Hz), 3.65 (2H, dd, ^2J = 8.9 Hz, ^3J = 6.6 Hz), 1.80 (m, 2H), 1.55 (m, 2H), 1.25 (m, 2H), 1.0 (6H, d, ^3J = 6.9 Hz), 0.95 (6H, tr, ^3J = 7.5 Hz); ^{13}C NMR ($CDCl_3$, 100 MHz) δ 153.4, 115.4, 73.6, 34.8, 26.1, 16.5, 11.3; FTIR (KBr, cm^{-1}) ν = 2961, 2930, 2876, 1508, 1467, 1390, 1228, 1045, 823; HRMS *m*/*z* calcd for $C_{16}H_{26}O_2$ 250.1933, found 250.1935.

1,4-Bis(2(*S*)-methoxypropoxy)benzene [*(SS)*-35] and *(RR)*-35. The diol (*SS*)-**19** (400 mg, 1.77 mmol) and *t*-BuOK (0.435 g, 3.89 mmol) were suspended in *t*-BuOH (6 mL). The mixture was stirred for 15 min at 30−40 °C, resulting in the formation of a clear yellow solution. MeI (2.28 g, 16.1 mmol) was added dropwise, giving immediate precipitation of KI. The suspension was stirred overnight, after which extra portions of *t*-BuOK (150 mg, 1.34 mmol) and MeI (1.0 g, 7.0 mmol) were added. Stirring was continued for another 2 h, after which the solvent was removed in vacuo. H_2O was added to the residue, and the suspension was extracted with CH_2Cl_2. The organic layer was dried ($MgSO_4$), filtered, and concentrated in vacuo. The crude product was purified by column chromatography (SiO_2, hexane/EtOAc (7:3)) to yield *(SS)*-**35** as a yellow clear oil (345 mg, 77%): $[\alpha]^{25}_D = -32.0°$ (*c* = 6.0 in Me_2CO); ^{1}H NMR ($CDCl_3$, 400 MHz) δ 6.85 (4H, s), 3.90 (2H, dd, ^2J = 9.6 Hz, ^3J = 5.9 Hz), 3.85 (2H, dd, ^2J = 9.9 Hz, ^3J = 4.5 Hz), 3.70 (2H, m), 3.45 (6H, s), 1.25 (6H, ^3J = 6.3 Hz); ^{13}C NMR ($CDCl_3$, 100 MHz) δ 153.1, 115.4, 75.3, 72.0, 56.9, 16.5; FTIR (KBr, cm^{-1}) ν = 2975, 2929, 2823, 1507, 1455, 1449, 1375, 1231, 1154, 1104, 1069, 1040, 825; HRMS *m*/*z* calcd for $C_{14}H_{22}O_4$ 254.1518, found 254.1519.

(RR)-**35** was prepared from the diol *(RR)*-**19** in a similar fashion to yield a yellow, clear oil in 70% yield. The spectroscopic data were identical with those reported for compound *(SS)*-**35**: $[\alpha]^{26}_D = +41.1°$ (*c* = 2.2 in Me_2CO).

1,4-Bis(2(*S*)-ethoxypropoxy)benzene [(*SS*)-36]. The diol (*SS*)-**19** (55 mg 0.24 mmol), KOH (95 mg 1.70 mmol), and EtI (227 mg, 1.46 mmol) were suspended in THF (2.5 mL). The mixture was stirred for 2 days at reflux, after which extra portions of KOH (35 mg, 0.63 mmol) and EtI (80 mg, 0.51 mmol) were added. The suspension was refluxed for another day. The solvent was removed in vacuo, H_2O was added to the residue, and the suspension was extracted with CH_2Cl_2. The organic layer was dried ($MgSO_4$), filtered, and concentrated in vacuo. The crude product was purified by column chromatography (CH_2Cl_2 and then hexane/EtOAc (5:1)) to yield (*SS*)-**36** as a yellow clear oil (65 mg, 90%): $[\alpha]^{20}_D = -16.6°$ (*c* = 1.63 in Me_2CO); ^{1}H NMR ($CDCl_3$, 400 MHz) δ 6.80 (4H, s), 3.90 (2H, dd, ^2J = 9.2 Hz, ^3J = 5.5 Hz), 3.80 (4H, m), 3.60 (4H, m), 1.30 (6H, d, ^3J = 6.3 Hz), 1.20 (6H, t, ^3J = 7.0 Hz); ^{13}C NMR ($CDCl_3$, 100 MHz) δ 153.2, 115.5, 73.6, 72.3, 64.6, 17.4, 15.6; FTIR (KBr, cm^{-1}) ν = 2974, 2928, 2871, 1508, 1456, 1374, 1230, 1154, 1107, 1067, 1044, 825; HRMS *m*/*z* calcd for $C_{16}H_{26}O_4$ 282.1831, found 282.1818.

1,4-Bis[2(*S*)-(2-methoxyethoxy)propoxy]benzene [*(SS)*-37]. The diol (*SS*)-**19** (79 mg, 0.35 mmol), KOH (135 mg, 2.41 mmol), and the tosylate of 2-methoxyethanol[22] (480 mg, 2.09 mmol) were suspended in THF (3 mL). The reaction mixture was stirred for 2 days at reflux, after which extra portions of KOH (45 mg, 0.80 mmol) and tosylate

(160 mg, 0.70 mmol) were added. The suspension was heated under reflux for another day. The solvent was removed in vacuo, H_2O was added to the residue, and the suspension extracted with CH_2Cl_2. The organic layer was dried ($MgSO_4$), filtered, and concentrated in vacuo. The crude product was purified by column chromatography (CH_2Cl_2 and hexane/EtOAc (3:1)) to yield an oil that still was not completely pure. Further purification by column chromatography (CH_2Cl_2/MeCOEt (10:1)) gave pure compound *(SS)*-**37** (64 mg, 54%): $[\alpha]^{20}_D = -11.6°$ ($c = 1.34$ in Me_2CO); ^{1}H NMR ($CDCl_3$, 400 MHz) δ 6.80 (4H, s), 4.00 (2H, dd, $^2J = 11.2$ Hz, $^3J = 7.5$ Hz), 3.85 (4H, m), 3.75 (4H, t, $^3J = 4.9$ Hz), 3.55 (4H, m), 3.40 (6H, s), 1.30 (6H, d, $^3J = 6.2$ Hz); ^{13}C NMR ($CDCl_3$, 100 MHz) δ 153.0, 115.4, 74.4, 72.2 (2), 68.7, 59.0, 17.3; FTIR (KBr, cm^{-1}) $\nu = 2974$, 2925, 2874, 1508, 1456, 1374, 1230, 1108, 1044, 826; GC/MS peaks at *m*/*z* 342 and 343 (2.4% and 0.4% abundance relative to 59).

^{1}H NMR Spectroscopic Studies of Complexation. Solutions with a 1:1 molar ratio of the π-electron-rich and π-electron-deficient components were prepared in CD_3CN with concentrations of 5×10^{-3} mol dm^{-3}. All chemical shift changes ($\Delta\delta$) for the 1:1 complexes are quoted in parts per million, and they were calculated using the equation $\Delta\delta = \delta$(observed) $- \delta$(free).

UV Spectrophotometric Titrations. The changes in the optical density of solutions of complexes were recorded as the relative concentrations of thread components of the complexes were increased with respect to the tetracationic cyclophane **1**·4PF_6. All stability constants were determined in dry MeCN solution at 298 K. In a typical experiment, a solution of **1**·4PF_6 was made up in a volumetric flask and its optical density recorded in a 1 cm path length cuvette. A known quantity of the guest was added to the solution. The optical density of this solution of the complex was recorded and the procedure repeated until no significant change in the optical density was observed when further guest was added. Molar ratios of threads to the tetracationic cyclophane employed were in the range 0.1:1 to 30:1 for strong 1:1 complexes and in the range 1:1 to 100:1 for weak 1:1 complexes. The data were treated with a nonlinear curve-fitting program (*UltraFit*; Biosoft: Cambridge, 1992) running on an Apple Macintosh microcomputer.

X-ray Crystallography. Single crystals suitable for X-ray crystallographic analysis of **5** were grown by vapor diffusion of *i*-Pr_2O into a solution of the compound **5** in $CHCl_3$. Single crystals of the [2]pseudorotaxanes **5/1**·4PF_6, *(SS)*-**30/1**·4PF_6, and *(SS)*-**37/1**·4PF_6 were grown by vapor diffusion of *i*-Pr_2O into 1:1 solutions of the appropriate components in MeCN. Table 3 provides a summary of the crystal data, data collection, and refinement parameters for **5** and the [2]pseudorotaxanes **5/1**·4PF_6, *(SS)*-**30/1**·4PF_6, and *(SS)*-**37/1**·4PF_6.

CD/UV Measurements. In all cases, **1**·4PF_6 was dissolved in MeCN with a few molar equivalents (between 1 and 10) of the chiral thread. Care was taken for the optical density of the solution to be between 0.1 and 1.5. Compounds (*SS*)-**19**, (*RR*)-**19**, (*RR*)-**20**, (*SS*)-**29**, (*RR*)-**29**, (*SS*)-**30**, (*SS*)-**31**, (*RR*)-**31**, (*SS*)-**34**, (*SS*)-**35**, (*RR*)-**35**, (*SS*)-**36**, and (*SS*)-**37** (15.2, 5.9, 7.5, 7.1, 6.9, 14.5, 9.0, 8.7, 76.0, 11.0, 15.5, 8.1 and 7.0 mg, respectively) with **1**·4PF_6 (10.0, 3.3, 4.2, 4.7, 4.3, 3.0, 2.9, 2.6, 15, 2.8, 3.8, 6.2, and 5.0 mg, respectively) were dissolved in MeCN (3.25, 1.59, 2.18, 1.55, 1.69, 1.90, 1.49, 1.45, 4.1 1.65, 1.71, 1.42, and 1.59 g, respectively). These clear solutions were investigated with UV and CD spectroscopy at room temperature. The λ_{max} values of the solutions were located at 474, 467, 460, 461, 464, 476, 469, 467, and 468 nm for **19**, **20**, **29**, **30**, **31**, **34**, **35**, **36**, and **37**, respectively, in the UV spectra. For the experiments shown in Figure 7 the following solutions were prepared: (Figure 7A) 7.1 mg of (*SS*)-**29**, 4.7 mg of **1**·4PF_6, 1.55 g of MeCN; 5.9 mg of (*RR*)-**29**, 4.3 mg of **1**·4PF_6, 1.69 g of MeCN; (Figure 7B) 15.2 mg of (*SS*)-**19**, 10 mg of **1**·4PF_6, 3.25 g of MeCN; 5.9 mg of (*RR*)-**19**, 3.3 mg of **1**·4PF_6, 1.59 g of MeCN. The variable temperature measurements (Figure 8) were performed with (Figure 8A) 7.1 mg of (*SS*)-**29**, 4.7 mg of **1**·4PF_6, and 1.67 g of MeCN and (Figure 8B) 15.2 mg of (*SS*)-**19**, 10 mg of **1**·4PF_6, and 3.25 g of MeCN. All solutions were measured in 1 cm sample holders.

Acknowledgment. We thank Henk Eding and Joost van Dongen for obtaining the elemental analyses and mass spectra, respectively. The research was supported by the CIBA-GEIGY Foundation (Japan) for the Promotion of Science and the Engineering and Physical Sciences Research Council in the United Kingdom. DSM Research is gratefully acknowledged for an unrestricted research grant to the Eindhoven Group in The Netherlands.

Supporting Information Available: Tables listing atomic coordinates, temperature factors, bond lengths and angles, and torsion angles and details of the refinement of the X-ray crystallographic data (38 pages). See any current masthead page for ordering information and Internet access instructions.

JA970018I